COHERENT ELASTIC NEUTRINO-NUCLEUS SCATTERING: STATUS AND PROSPECTS

Francesca Dordei
INFN Cagliari
Invisibles 2021 Workshop, 1 June 2021

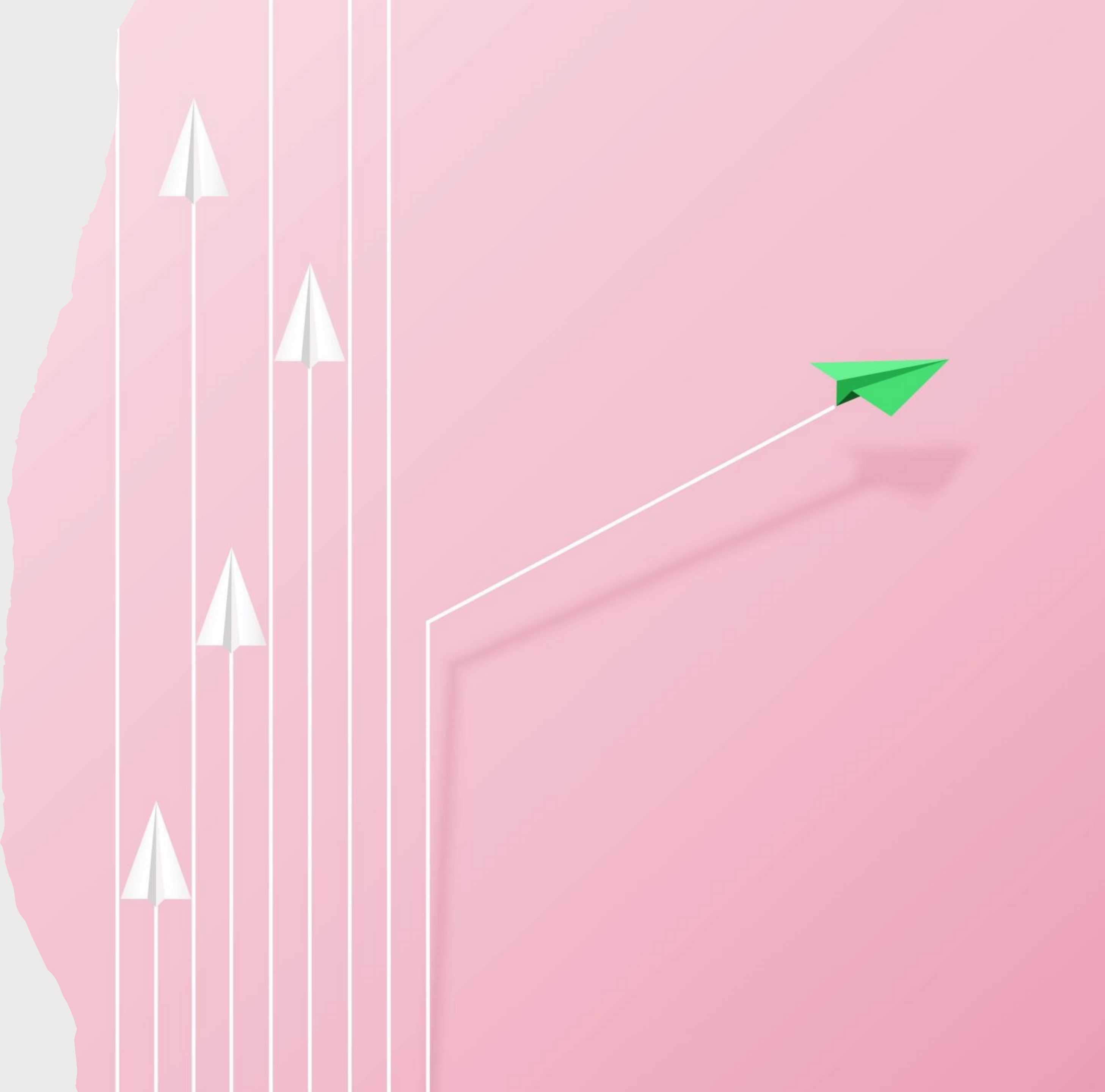

WHAT IS CEνNS?

- ***Coherent elastic neutrino-nucleus scattering (CEνNS):*** A neutrino scatters off a nucleus via exchange of a Z, and the nucleus recoils as a whole

$$\boldsymbol{\nu_\alpha + (A,Z) \rightarrow \nu_\alpha + (A,Z)}$$

- Predicted in 1974 by Freedman

- It took more than 40 years to finally measure nuclear recoils originating from this neutrino interaction!

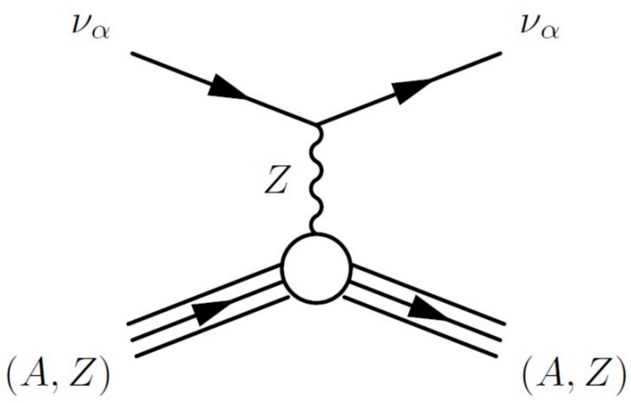

PHYSICAL REVIEW D VOLUME 9, NUMBER 5 1 MARCH 1974

Coherent effects of a weak neutral current

Daniel Z. Freedman†
National Accelerator Laboratory, Batavia, Illinois 60510
and Institute for Theoretical Physics, State University of New York, Stony Brook, New York 11790

(Received 15 October 1973; revised manuscript received 19 November 1973)

If there is a weak neutral current, then the elastic scattering process $\nu + A \rightarrow \nu + A$ should have a sharp coherent forward peak just as $e + A \rightarrow e + A$ does. Experiments to observe this peak can give important information on the isospin structure of the neutral current. The experiments are very difficult, although the estimated cross sections (about 10^{-38} cm^2 on carbon) are favorable. The coherent cross sections (in contrast to incoherent) are almost energy-independent. Therefore, energies as low as 100 MeV may be suitable. Quasi-coherent nuclear excitation processes $\nu + A \rightarrow \nu + A^*$ provide possible tests of the conservation of the weak neutral current. Because of strong coherent effects at very low energies, the nuclear elastic scattering process may be important in inhibiting cooling by neutrino emission in stellar collapse and neutron stars.

Our suggestion may be an act of hubris, because the inevitable constraints of interaction rate, resolution, and background pose grave experimental difficulties for elastic neutrino-nucleus scattering. We will discuss these problems at the end of this note, but first we wish to present the theoretical ideas relevant to the experiments.

LOW-ENERGY REGIME

Coherent elastic neutrino-nucleus scattering

Interactions with nuclei and electrons, minimally disruptive of the nucleus

Interactions with nucleons inside nuclei, often disruptive, hadroproduction

Deep Inelastic Scattering

keV MeV GeV TeV PeV

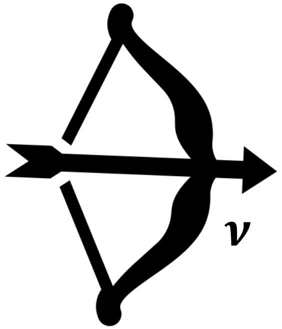

COHERENCE MEANS…

Nucleon wavefunctions in the target nucleus are in phase with each other at low momentum transfer.

The interaction is coherent up to neutrino energies $E_\nu \sim 50$ MeV for medium size nuclei.

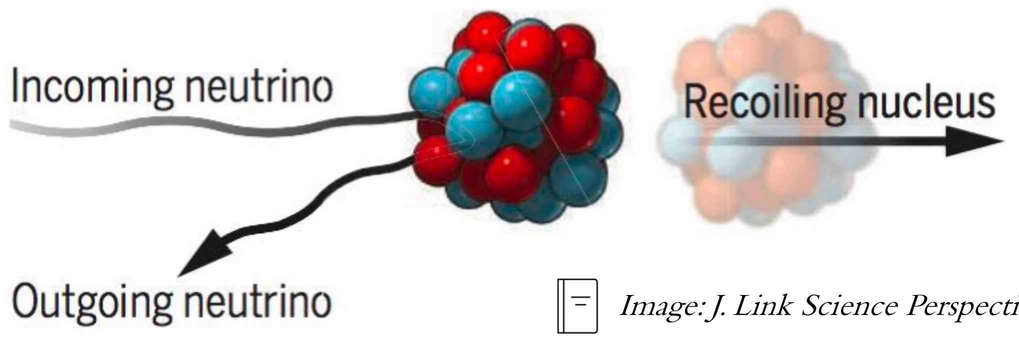

Image: J. Link Science Perspectives

For $q \cdot R \ll 1$:

Three-momentum transfer $\quad$ Nuclear radius

$q = \sqrt{2 m_N E_r}$

$$\frac{d\sigma^{CE\nu NS}(E_\nu, E_r)}{dE_r} \cong \frac{G_F^2}{4\pi} Q_w^2 \, m_N \left(1 - \frac{m_N E_r}{2E_\nu^2}\right) |F(E_r)|^2$$

where $Q_w = N - (1 - 4\sin^2\theta_W)\, Z$

as $\sin^2\theta_W$ is about 1/4, the second term is close to zero and the cross section ***scales with the number of neutrons squared*** $\sigma \propto N^2$.

AN ACT OF HUBRIS

The cross section is rather large for the neutrino world...

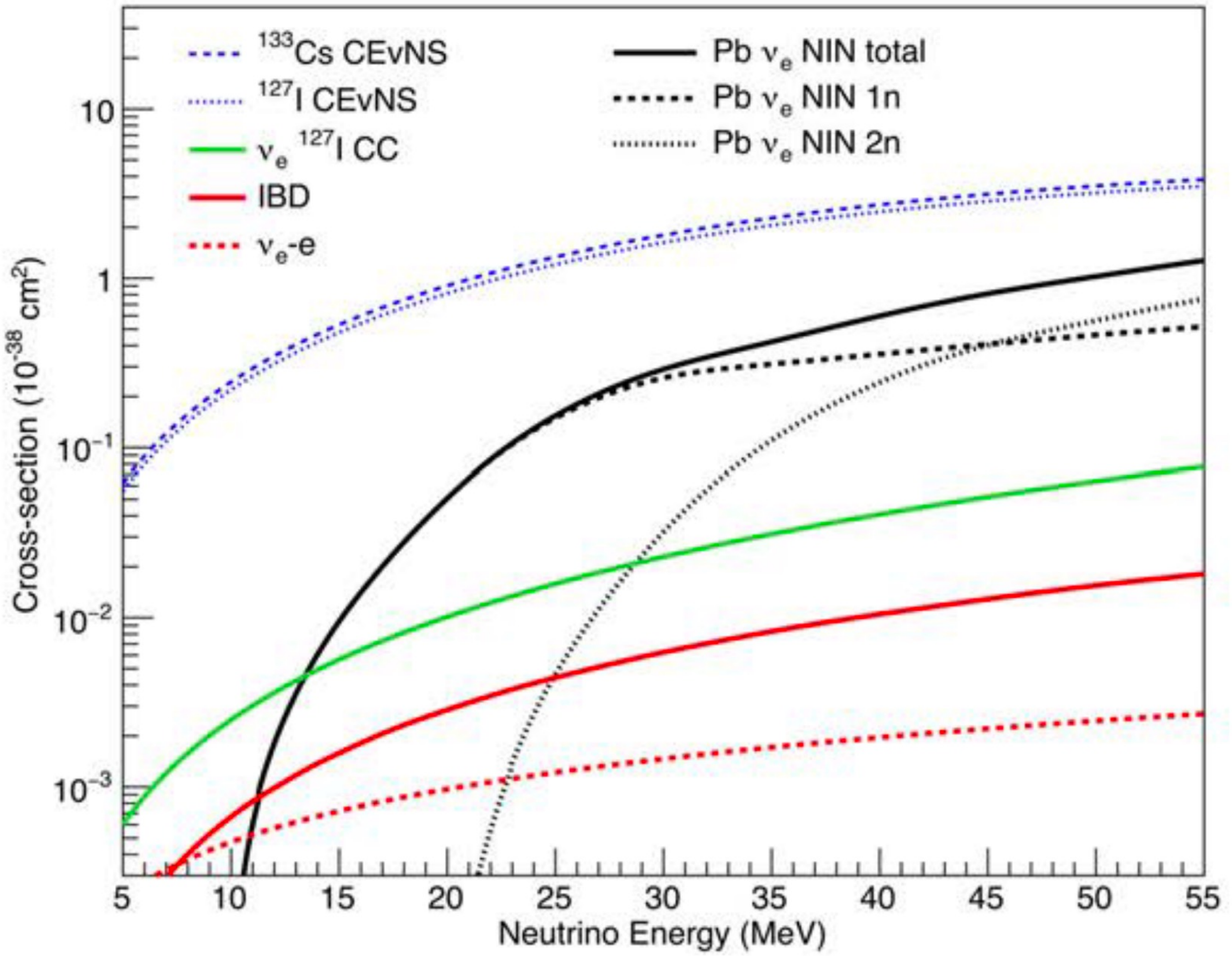

D. Akimov et al. ***Science*** 357.6356 (2017)

AN ACT OF HUBRIS

...However hard to observe due to ***tiny nuclear recoil energies***:

$$q \ll \frac{1}{R}$$

The maximum nuclear recoil energy for a target nucleus of mass m_N is given by

$$E_r^{max} \cong \frac{2E_\nu^2}{m_N + 2E_\nu}$$

which is in the ***keV range*** for $E_\nu \sim 50$ MeV.
(For caesium nuclei $E_r^{max} \approx 40$ keV)

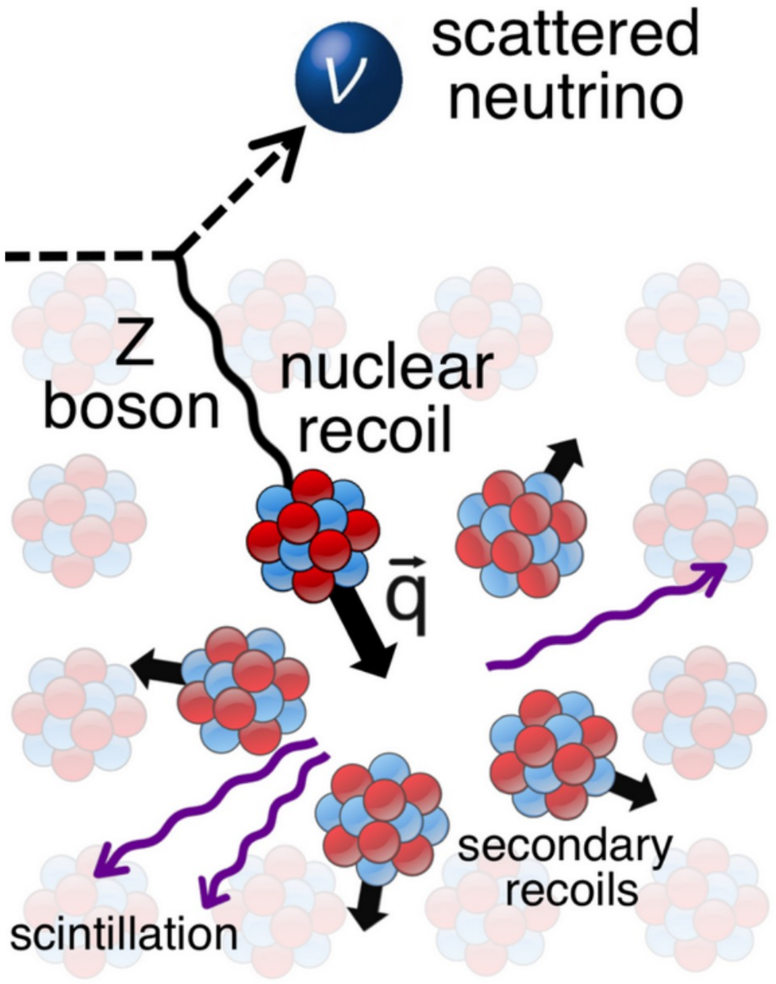

AN ACT OF HUBRIS

…However hard to observe due to ***tiny nuclear recoil energies***:

$$q \ll \frac{1}{R}$$

The maximum nuclear recoil energy for a target nucleus of mass m_N is given by

$$E_r^{max} = \frac{2E_\nu^2}{m_N + 2E_\nu}$$

which is in the ***keV range*** for $E_\nu \sim 50$ MeV. (For caesium nuclei $E_r^{max} \approx 40$ keV)

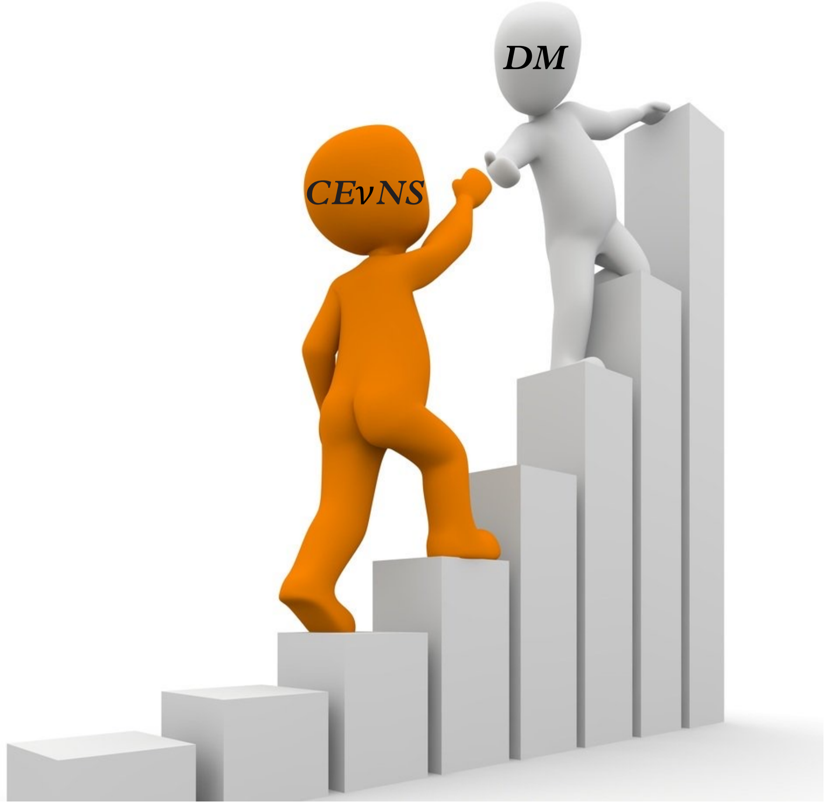

These energies are below the typical detection threshold of the conventional large neutrino detectors (~MeV).
Dark matter detector developed over the last decade are ***sensitive to ~keV to 10's of keV recoils***!

SOURCE REQUIREMENTS

Need an appropriate source of neutrinos (high flux, well understood, pulsed for background rejection, multiple flavors, etc).

Two types of neutrino sources are considered in experiments

At a spallation neutron source, where the neutrinos are produced from the decay of pions/muons

At nuclear reactors, where the neutrinos are produced in beta decays of fissions fragments

Moreover, shielding from natural radioactivity or source-induced backgrounds is required.

THE COHERENT EXPERIMENT - SNS

The ***Spallation Neutron Source*** @Oak Ridge

- 1GeV protons hit liquid-Hg target
- Recently reached 1.4MW
- Pulsed @60Hz: measure steady-state bkg out of beam!
- Pion-decay-at-rest neutrino source
- Multi-target program to measure N^2 dependence

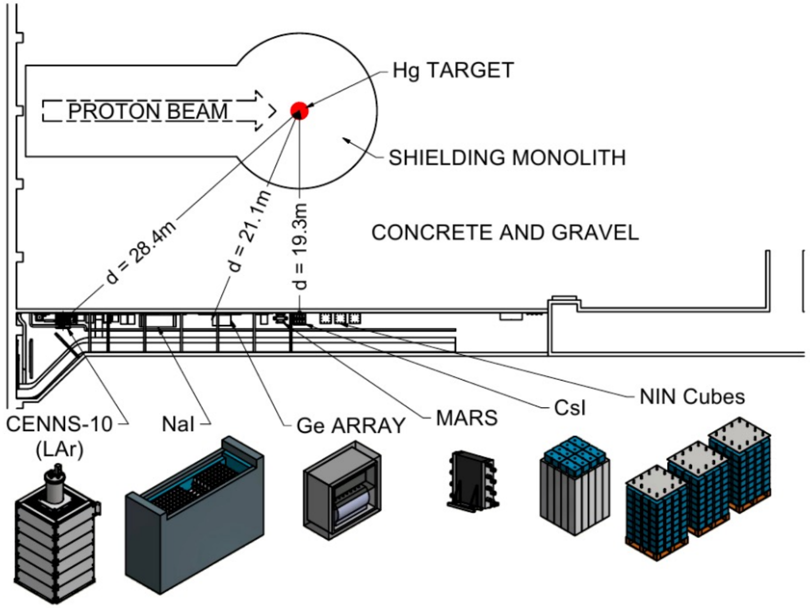

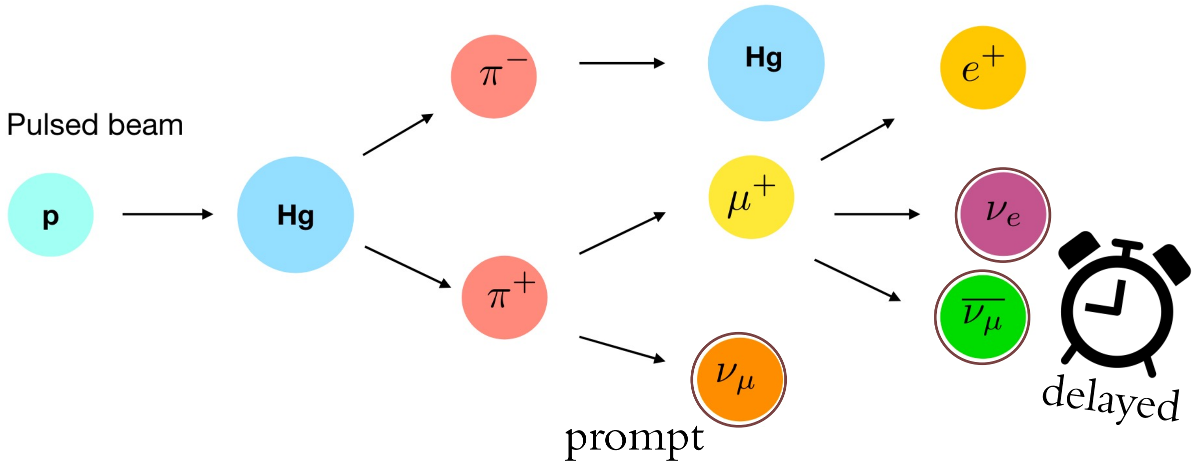

Figure from J. Gehrlein

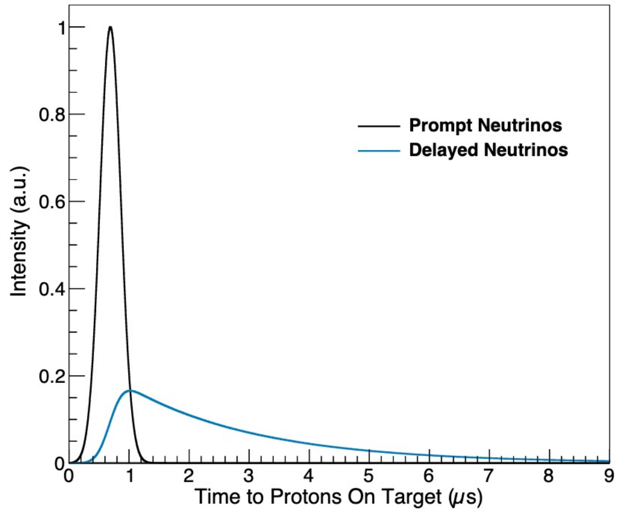

COHERENT AT THE SNS: CsI

- First CsI result 2017!
- First CEνNS detection with 14.6 kg CsI scintillating crystal
- 19.3 m from the source
- ***134 ± 22 CEνNS*** events: 6.7σ significance
- To be compared with prediction: ***173 ± 48*** events

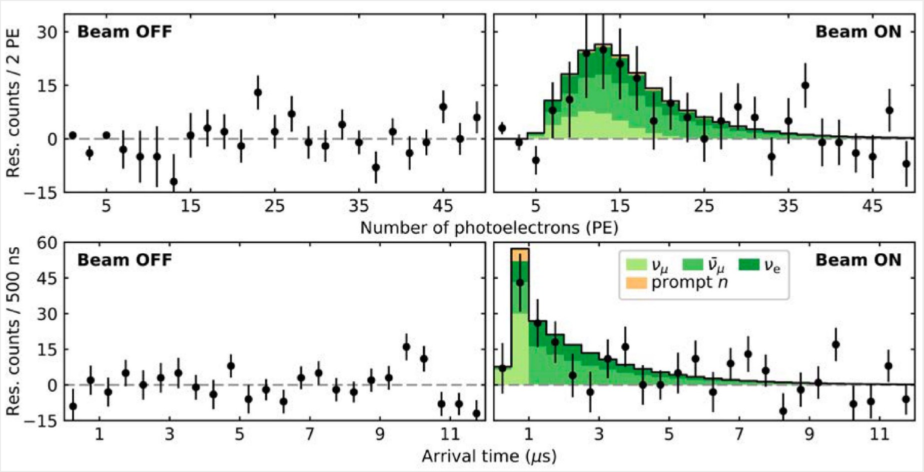

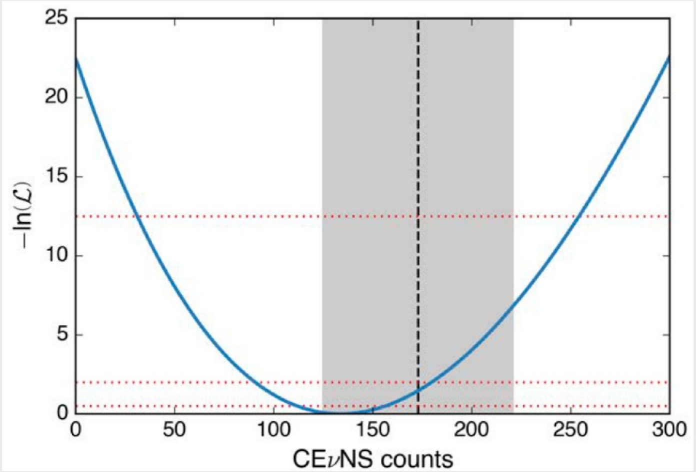

D. Akimov et al. ***Science*** 357.6356 (2017)

COHERENT CsI 2020

- Increased statistics. More than 2x!
- 2D Likelihood fit in numbers of photoelectrons and reconstructed time.

No-CEνNS rejection	*11.6σ*
SM CEνNS prediction	333±11(th)±42(ex)
Fit CEνNS events	306±20
Fit χ^2/dof	82.4/98
CEνN cross section	$169^{+30}_{-26} \times 10^{-40}$ cm^2
SM cross section	$189 \pm 6 \times 10^{-40}$ cm^2

- Result is consistent with SM prediction at 1σ
- Flux uncertainty now dominates the systematic uncertainty.
- Overall systematic uncertainty reduced: 28% →13%

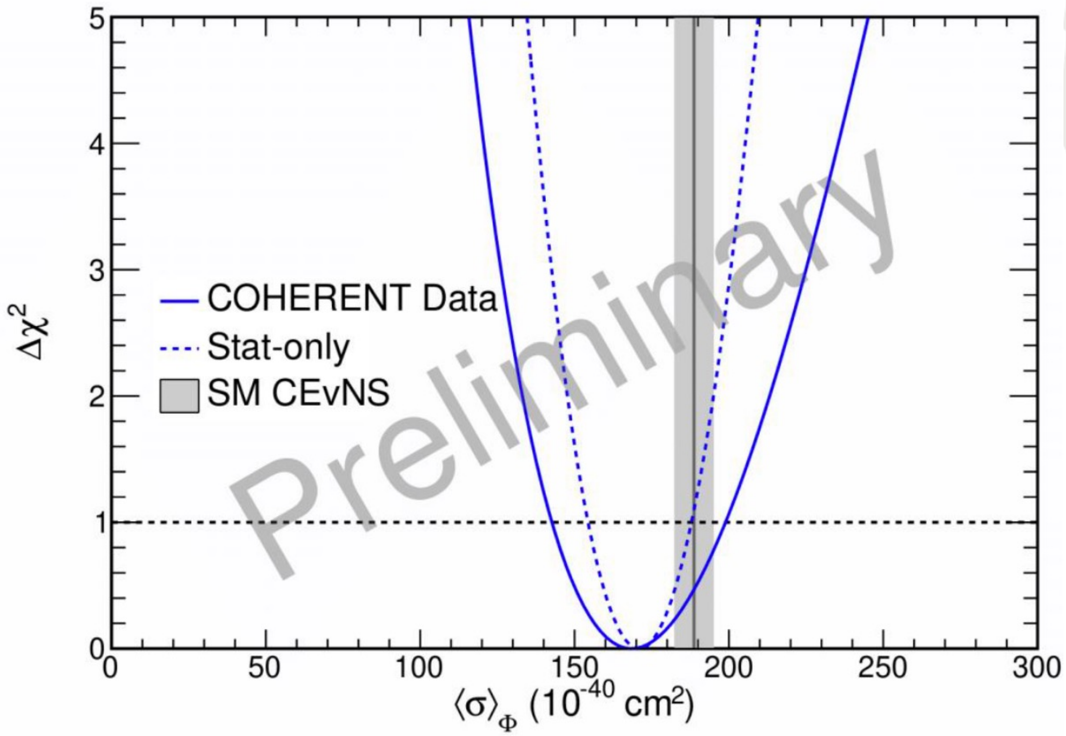

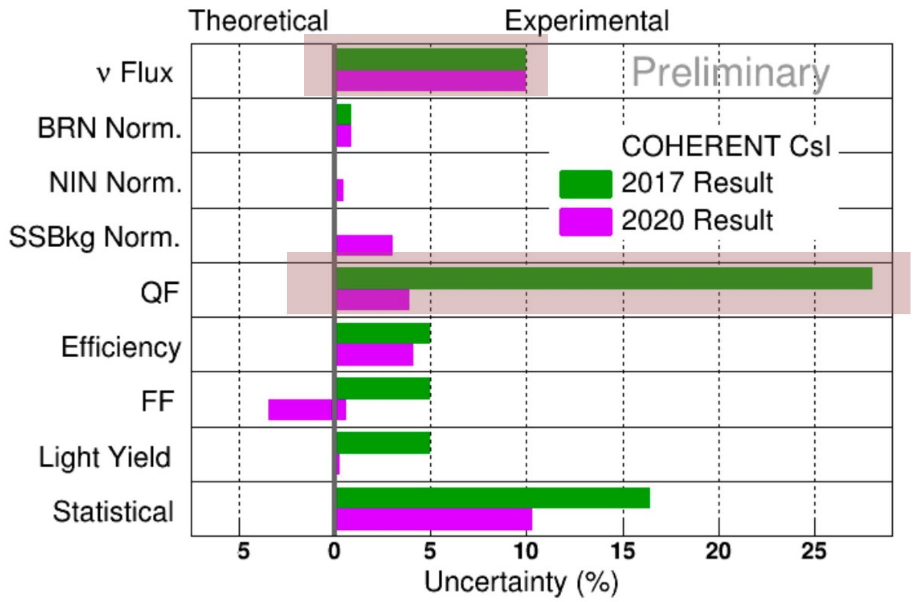

COHERENT Collaboration, talks @Magnificent CEνNS '20

COHERENT IN ARGON

- 2020 first results using Ar, aka CENNS-10.
- 27.5 m from the SNS target.
- Active mass of 24 kg of atmospheric argon
- Single phase only (scintillation), thr. 20 keV_{nr}

>3σ CEνNS detection significance

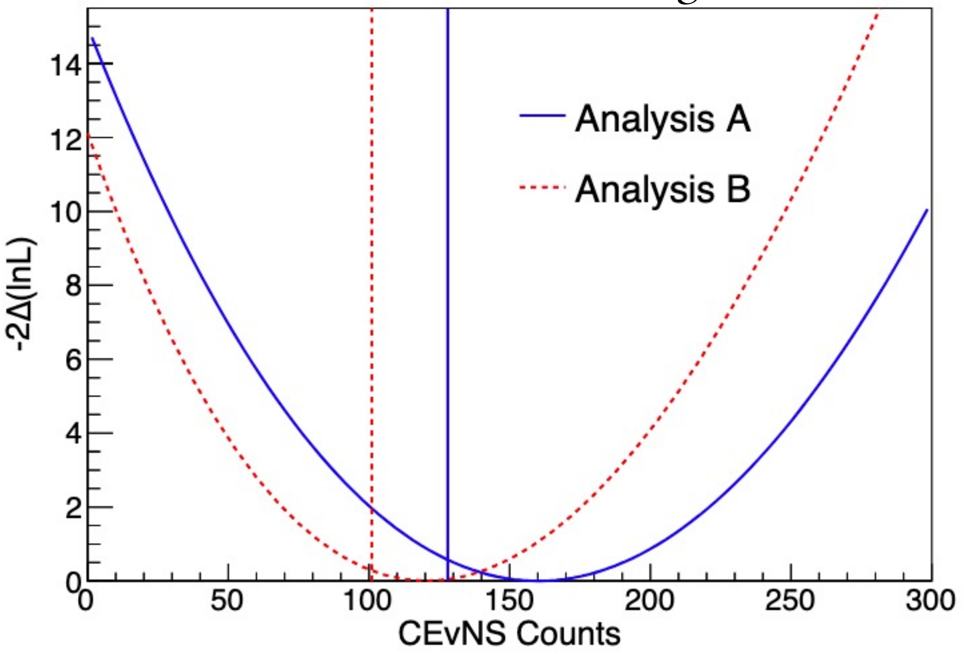

COHERENT, PRL 126, 012002 (2021)

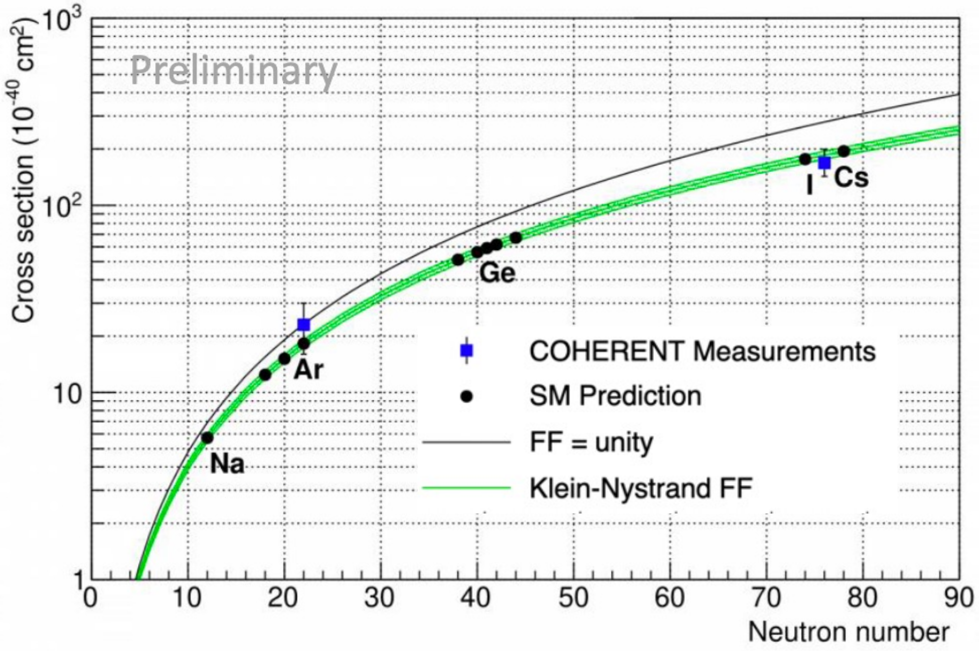

Pershey, talk @Magnificent CEνNS '20

Observed cross section consistent with N^2 dependence

CENNS-10 continues data taking and 5σ significance should be reached with the data up to end of 2020.

ONGOING AND FUTURE EXPERIMENTS

- Several ongoing experimental effort exploiting different materials and sources
- New results by several collaborations expected soon

See B. Mauri, NUCLEUS outer veto prototype for the CEνNS detection at nuclear reactors, PhD Forum @Invisible2021

Konovalov, talk @Magnificent CEνNS

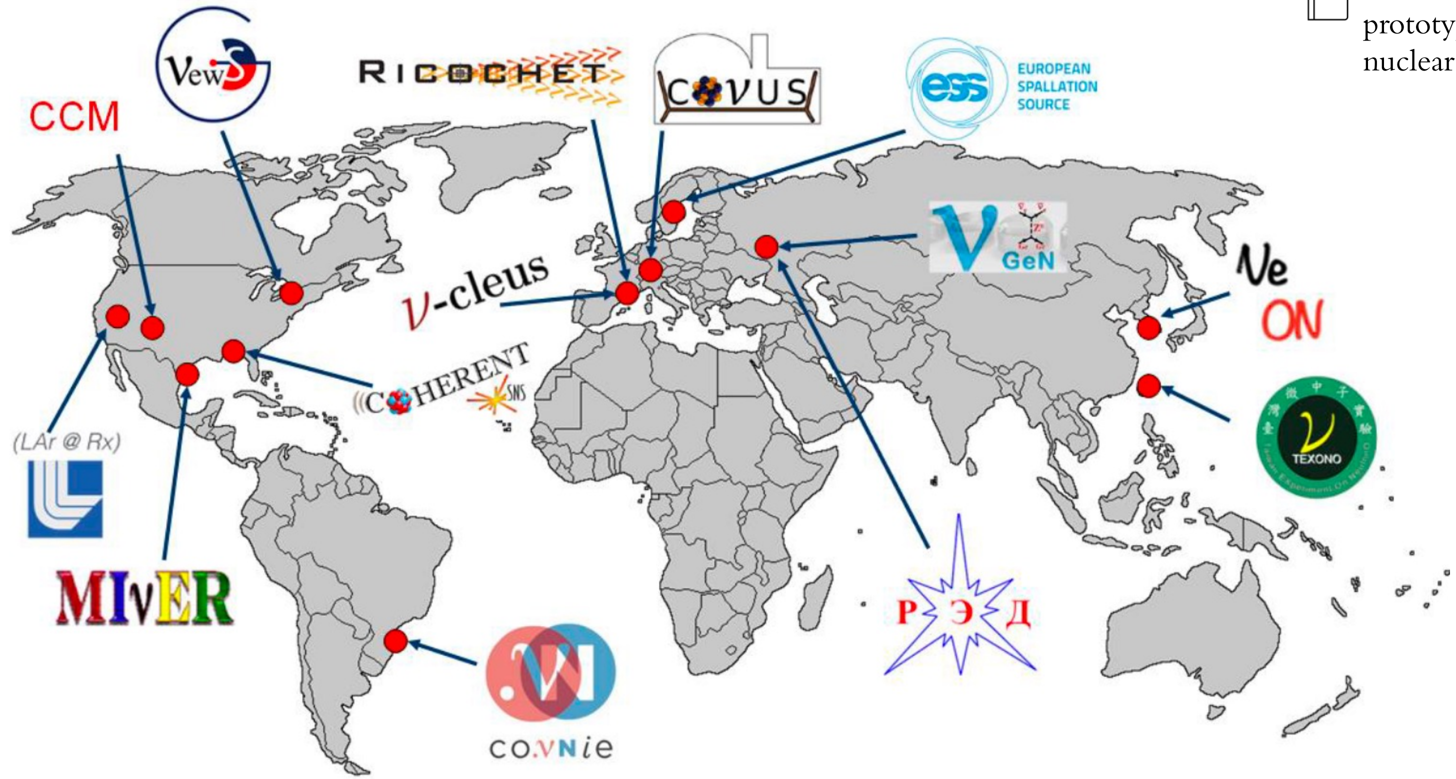

CEνNS search and study experiments around the world

COνUS

- Experiment @ the Brokdorf nuclear power plant in Germany, ~17 m from the core
- Flux of more than $10^{13}s^{-1}cm^{-2}$ at the experimental site
- E_ν< 10MeV and tiny recoils → Low threshold
- Reactor off periods allows to study the surrounding background
- Four 1 kg low-background ***germanium crystals*** installed inside a multilayer shield

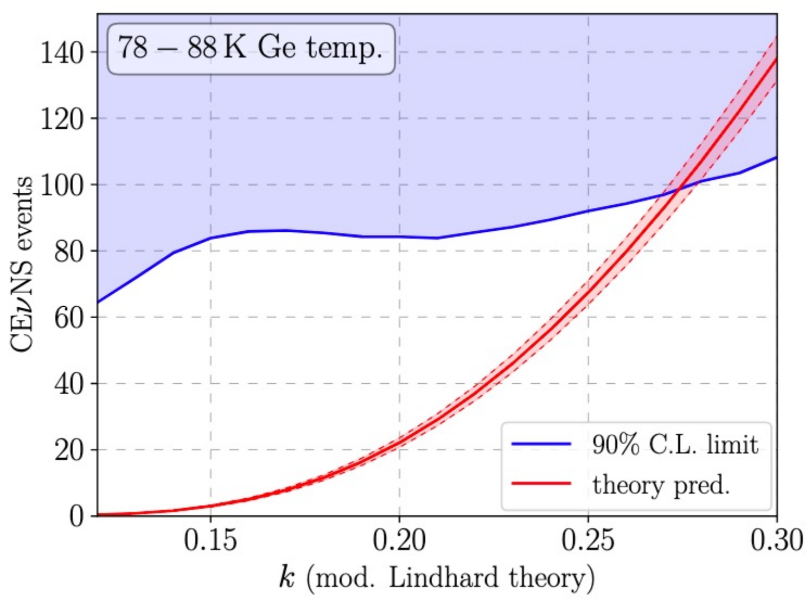

Best limit on CEνNS by reactor $\bar{\nu}$ in the fully coherent regime (presented as a function of the quenching parameter *k*)

- k > 0.27 disfavored by data

Conus, PRL 126, 041804 (2021)

WHAT CAN WE LEARN FROM CEνNS?

WHAT CAN WE LEARN FROM CEνNS?

$$\frac{d\sigma^{CE\nu NS}(E_\nu, E_r)}{dE_r} \cong \frac{G_F^2\, m_N}{\pi}\left(1 - \frac{m_N E_r}{2E_\nu^2}\right)\left[\boldsymbol{g_V^p}\left(\sin^2(\vartheta_W)\right) Z \boldsymbol{F_Z}(|\vec{\boldsymbol{q}}|^2) + \boldsymbol{g_V^n} N \boldsymbol{F_N}(|\vec{\boldsymbol{q}}|^2)\right]^2$$

Neutrino energy

Nuclear recoil energy

Mass of the nucleus

SM vector proton coupling

$g_V^p(\nu_e) = 0.0401,$
$g_V^p(\nu_\mu) = 0.0318,$
$g_V^n = -0.5094.$

SM vector neutron coupling

Weinberg angle

Proton Form Factor

Neutron Form Factor

WHAT CAN WE LEARN FROM CEνNS?

Neutrino energy

Mass of the nucleus

SM vector proton coupling

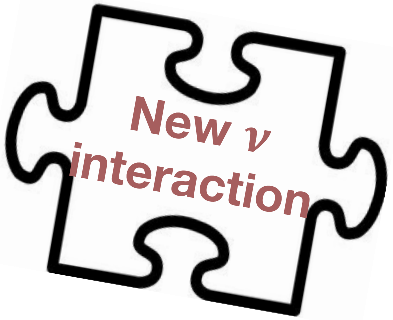

SM vector neutron coupling

$$\frac{d\sigma^{CE\nu NS}(E_\nu, E_r)}{dE_r} \cong \frac{G_F^2\, m_N}{\pi}\left(1 - \frac{m_N E_r}{2E_\nu^2}\right)\left[g_V^p\left(\sin^2(\vartheta_W)\right) Z F_Z(|\vec{q}|^2) + g_V^n N F_N(|\vec{q}|^2)\right]^2 + \dots$$

Nuclear recoil energy

Weinberg angle

Proton Form Factor

Neutron Form Factor

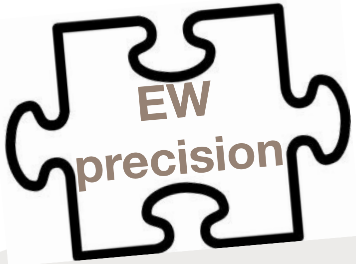

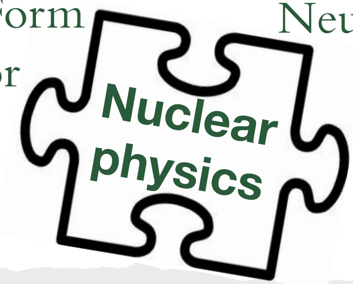

NEUTRON DISTRIBUTION RADIUS IN CsI

- The Z boson couples mostly with neutrons, so information on the neutron distribution can be obtained, which is very difficult to measure.
- Indeed, e scattering and μ spectroscopy can probe only the proton distribution.
- The information of R_n is encapsulated in the form factor $\boldsymbol{F_N(|\vec{q}|^2)}$.

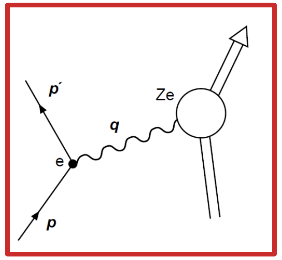

Cadeddu et al., arXiv:2102.06153

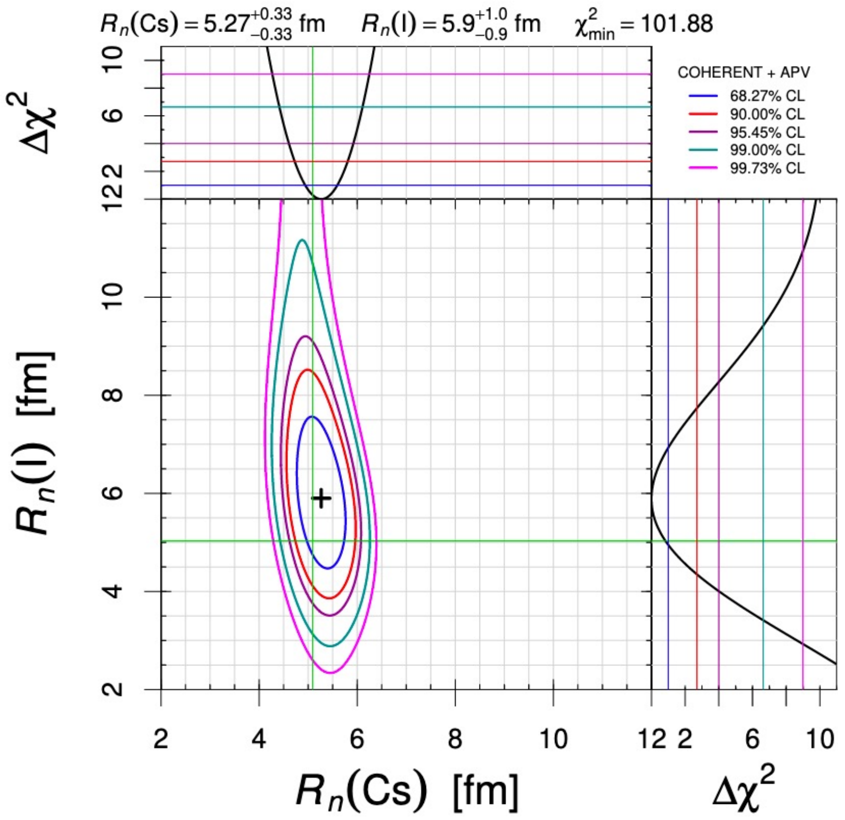

COHERENT + APV(Cs)

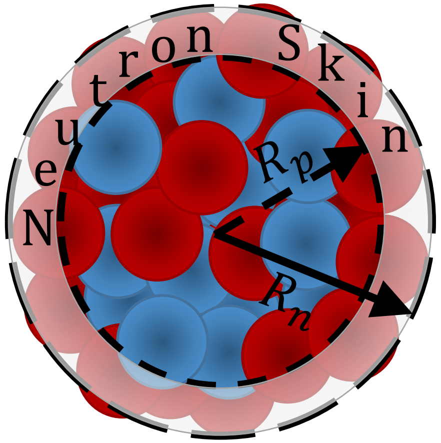

Figure from M. Cadeddu

$$\Delta R_{np}(^{133}\mathrm{Cs}) = R_n - R_p = 0.45^{+0.33}_{-0.33}\mathrm{fm}$$

$$\Delta R_{np}(^{127}\mathrm{I}) = R_n - R_p = 1.1^{+1.0}_{-0.9}\mathrm{fm}$$

Theoretical values with Skyrme-Hartree-Fock (SHF) and relativistic mean field (RMF) nuclear models :

	CsI		
Model	R_p	R_n	$R_n - R_p$
SHF SkM* [26]	4.73	4.86	0.13
SHF SkP [27]	4.75	4.87	0.12
SHF SkI4 [28]	4.70	4.83	0.14
SHF Sly4 [29]	4.73	4.87	0.13
SHF UNEDF1 [30]	4.71	4.87	0.15
RMF NL-SH [31]	4.71	4.89	0.18
RMF NL3 [32]	4.72	4.92	0.20
RMF NL-Z2 [33]	4.76	4.97	0.21

See also:
Cadeddu et al., PRL 120, 072501 (2018)
Cadeddu et al., PRD 101, 033004 (2020)
Papoulias, PRD 102, 113004 (2020)
Khan and Rodejohann, PRD 100, 113003 (2019)
Coloma et al, JHEP 08:030 (2020)
Aristizabal Sierra et al., JHEP 6, 141 (2019)

NEUTRON DISTRIBUTION RADIUS IN Ar

- The Z boson couples mostly with neutrons, so information on the neutron distribution can be obtained, which is very difficult to measure.
- Indeed, e scattering and μ spectroscopy can probe only the proton distribution
- The information of R_n is encapsulated in the form factor $\boldsymbol{F_N(|\vec{q}|^2)}$.

See also:
Payne et al., PRC 100, 061304 (2019)

Cadeddu et al., PRD 102, 015030 (2020)

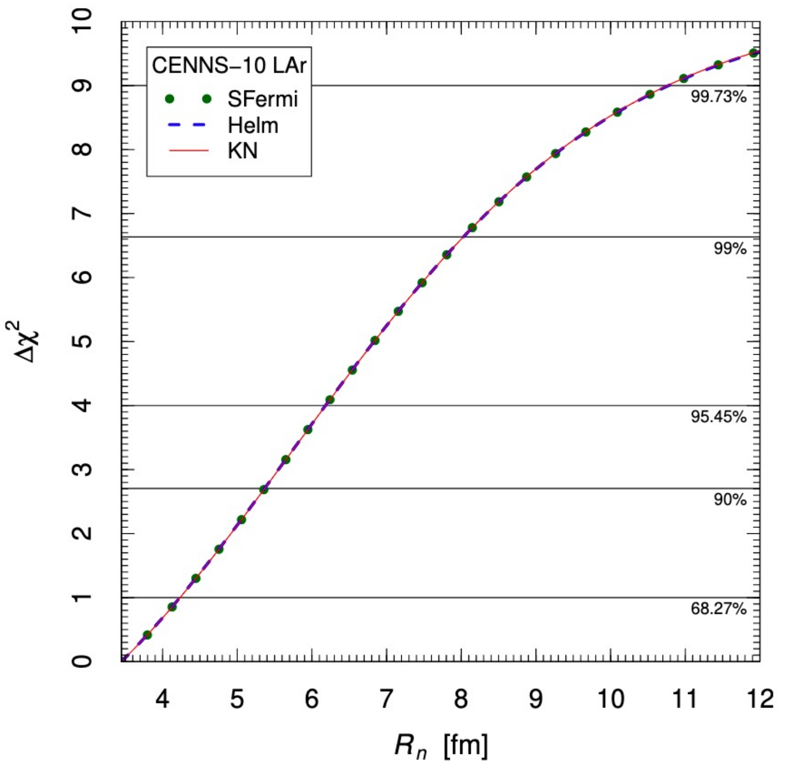

COHERENT ONLY

$R_n(^{40}\text{Ar}) < 4.2(1\sigma), 6.2(2\sigma), 10.8(3\sigma)$ fm

More statistics needed.

See also:
Miranda et al., JHEP 05 (2020) 130

$R_n(^{40}\text{Ar}) < 4.33$ fm @90% CL

Theoretical values with Sky3D nuclear models :

Interaction	R_p^{point}	R_n^{point}
Sky3D		
SkI3 [37]	3.33	3.43
SkI4 [37]	3.31	3.41
Sly4 [38]	3.38	3.46
Sly5 [38]	3.37	3.45
Sly6 [38]	3.36	3.44
Sly4d [39]	3.35	3.44
SV-bas [40]	3.33	3.42
UNEDF0 [41]	3.37	3.47
UNEDF1 [42]	3.33	3.43
SkM* [43]	3.37	3.45
SkP [44]	3.40	3.48

Important complementarity of R_n with the astrophysical sector

Reed at al., PRL 126, 172503 (2021)
Horowitz et al., PRL 86, 5647 (2001)
Cadeddu et al., arXiv:2102.06153

WEINBERG ANGLE

The dependence of the weak charge on the Weinberg angle allows CEνNS to measure it

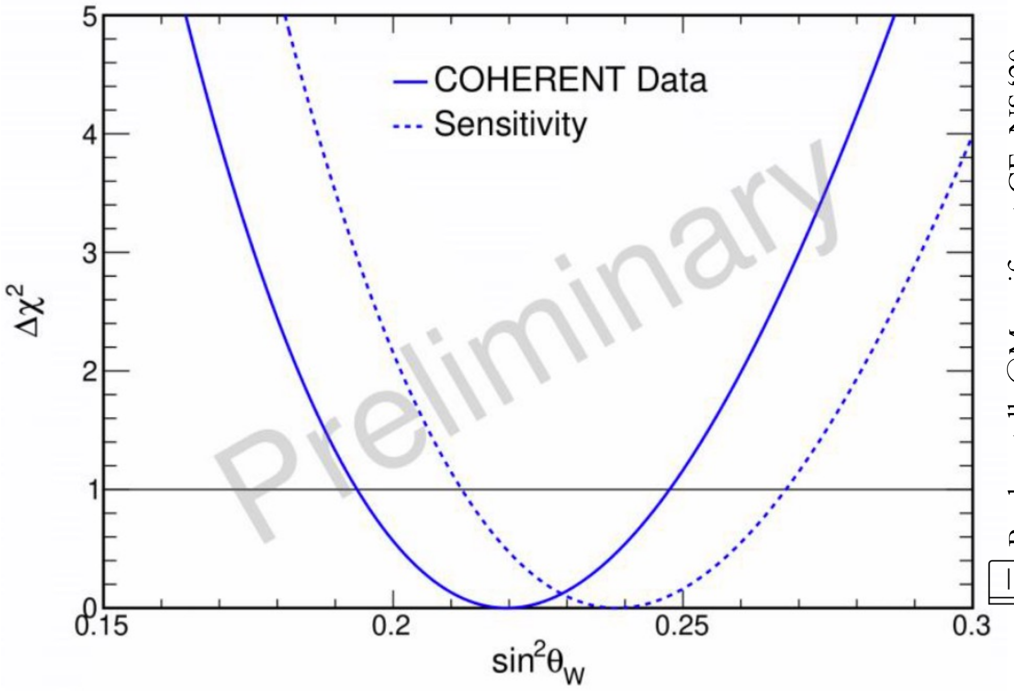

Pershey, talk @Magnificent CEνNS '20

$$\sin^2(\vartheta_W) = 0.220^{+0.028}_{-0.027}$$

Measurement not currently competitive due to the suppression of the proton contribution

However, CEνNS is helpful in combination with APV measurement on ^{133}Cs in order to provide experimental constrain on R_n and $\sin^2(\vartheta_W)$ simultaneously.

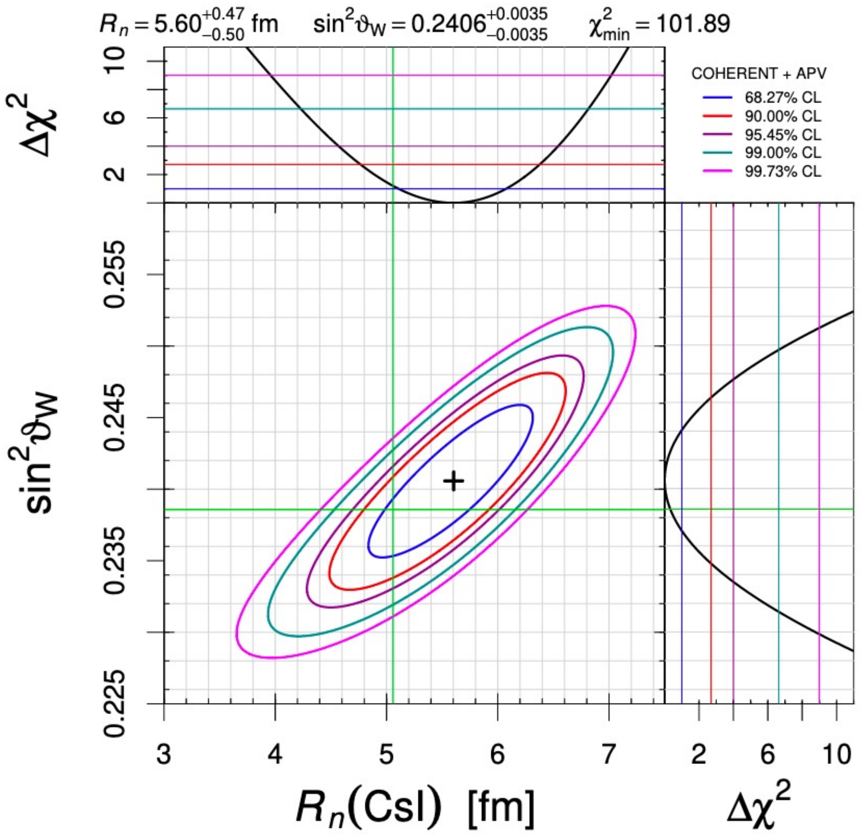

Cadeddu et al, arXiv:2102.06153

WEINBERG ANGLE

EW precision

The dependence of the weak charge on the Weinberg angle allows CEνNS to measure it

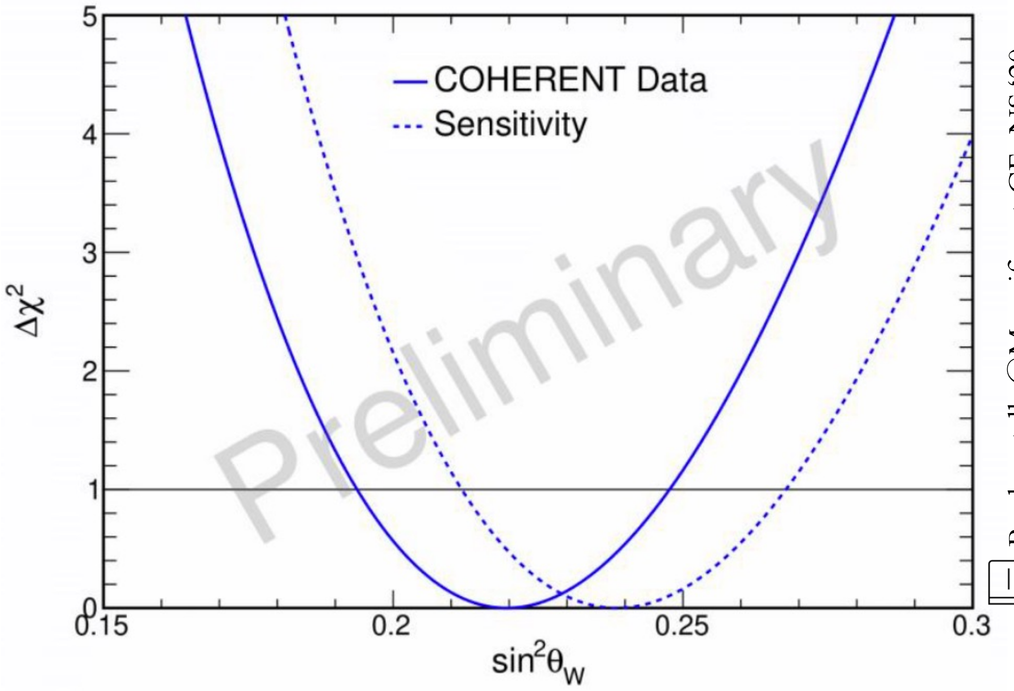

Pershey, talk @Magnificent CEνNS '20

$$\sin^2(\vartheta_W) = 0.220^{+0.028}_{-0.027}$$

Measurement not currently competitive due to the suppression of the proton contribution

However, CEνNS is helpful in combination with APV measurement on ^{133}Cs in order to provide experimental constrain on R_n and $\sin^2(\vartheta_W)$ simultaneously.

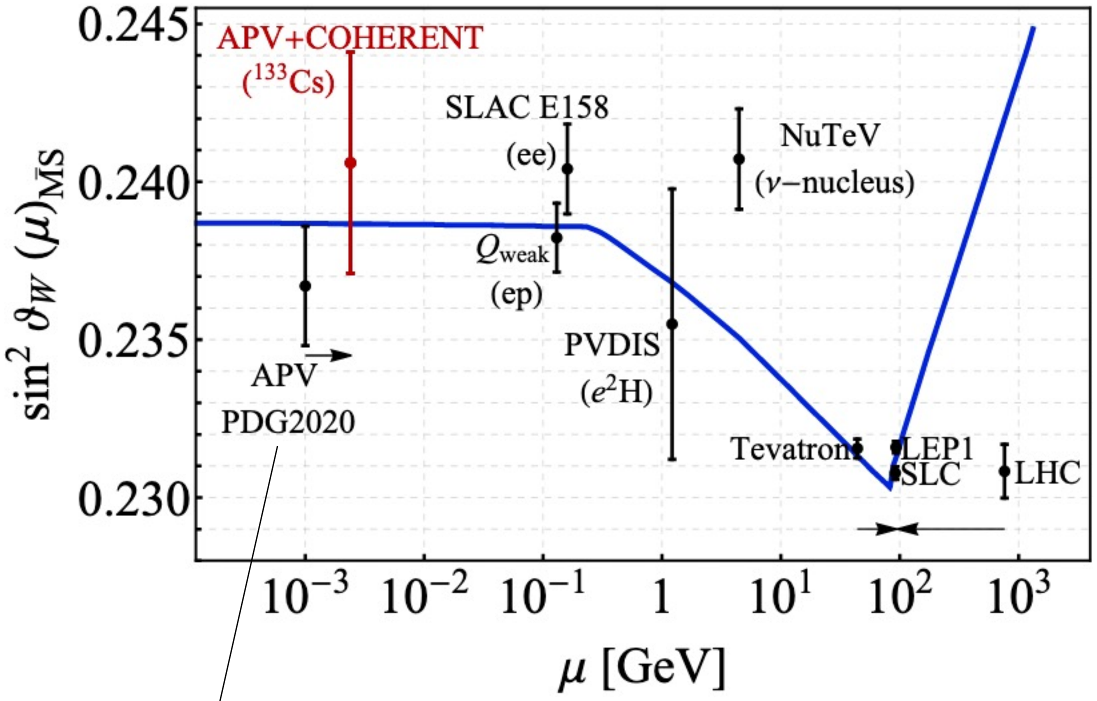

Cadeddu et al, arXiv:2102.06153

Here the value of $R_n(^{133}\mathrm{Cs})$ was extrapolated from hadronic experiments using antiprotonic atoms, known to be affected by considerable model dependencies.

New ν interaction

HEAVY VS LIGHT NSI MEDIATORS

One can consider vector neutral-current neutrino non-standard interactions

C. Giunti, PRD 101, 035039 (2020)
J. Barranco et al, JHEP 0512:021 (2005)

$$\frac{d\sigma^{CE\nu NS}(E_\nu, E_r)}{dE_r} \cong \frac{G_F^2\, m_N}{\pi}\left(1 - \frac{m_N E_r}{2E_\nu^2}\right) Q_\alpha^2 \quad \text{where}$$

$$Q_\alpha^2 = \left[\left(g_V^p + 2\varepsilon_{\alpha\alpha}^{uV} + \varepsilon_{\alpha\alpha}^{dV}\right) Z F_Z(|\vec{q}|^2) + \left(g_V^n + \varepsilon_{\alpha\alpha}^{uV} + 2\varepsilon_{\alpha\alpha}^{dV}\right) N F_N(|\vec{q}|^2)\right]^2 + \sum_{\beta\neq\alpha}\left|\left(2\varepsilon_{\alpha\beta}^{uV} + \varepsilon_{\alpha\beta}^{dV}\right) Z F_Z(|\vec{q}|^2) + \left(\varepsilon_{\alpha\beta}^{uV} + 2\varepsilon_{\alpha\beta}^{dV}\right) N F_N(|\vec{q}|^2)\right|^2$$

@COHERENT no sensitivity to $\varepsilon_{\tau\tau}$.

where $\varepsilon_{\alpha\beta}^{fV}$=size of NSI relative to SM

«Heavy» mediator

$$q^2 \ll M_{Z'} \rightarrow \varepsilon_{\ell\ell}^{fV} \propto \frac{g_{Z'}^2 Q_\ell' Q_f'}{M_{Z'}^2}$$

Effective four fermion interaction Lagrangian. The parameters ε describe the size of NSI relative to standard neutral-current weak interactions.

«Above ~ 1 GeV»

$$\varepsilon_{\ell\ell}^{fV} = \frac{g_{Z'}^2 Q_\ell' Q_f'}{\sqrt{2} G_F\left(|\vec{q}|^2 + M_{Z'}^2\right)}$$

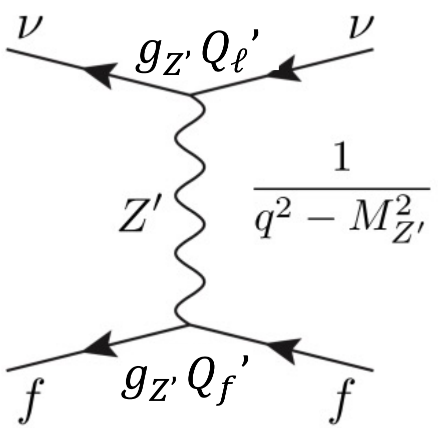

«Light» mediator

$$q^2 \gg M_{Z'} \rightarrow \varepsilon_{\ell\ell}^{fV} \propto \frac{g_{Z'}^2 Q_\ell' Q_f'}{|\vec{q}|^2}$$

One can assume the existence of U'(1) with an additional vector Z' or a scalar ϕ. One has also an explicit dependence on momentum transfer and Q charges.

«Above ~10 MeV»

New ν interaction

LIGHT MEDIATORS

Limits on different Z' light mediator models combining CsI and argon COHERENT data.

M. Cadeddu et al, JHEP 01 (2021) 116

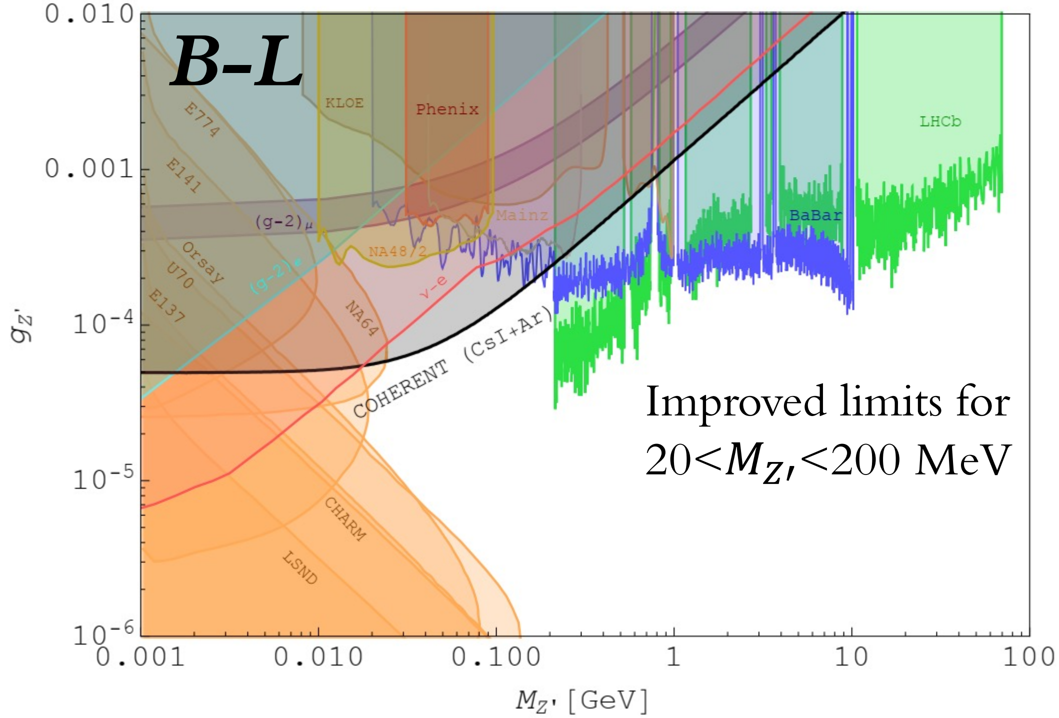

Complementarity with ν oscillation data!

P. Coloma et al, JHEP 01 (2021) 114
(Backup)

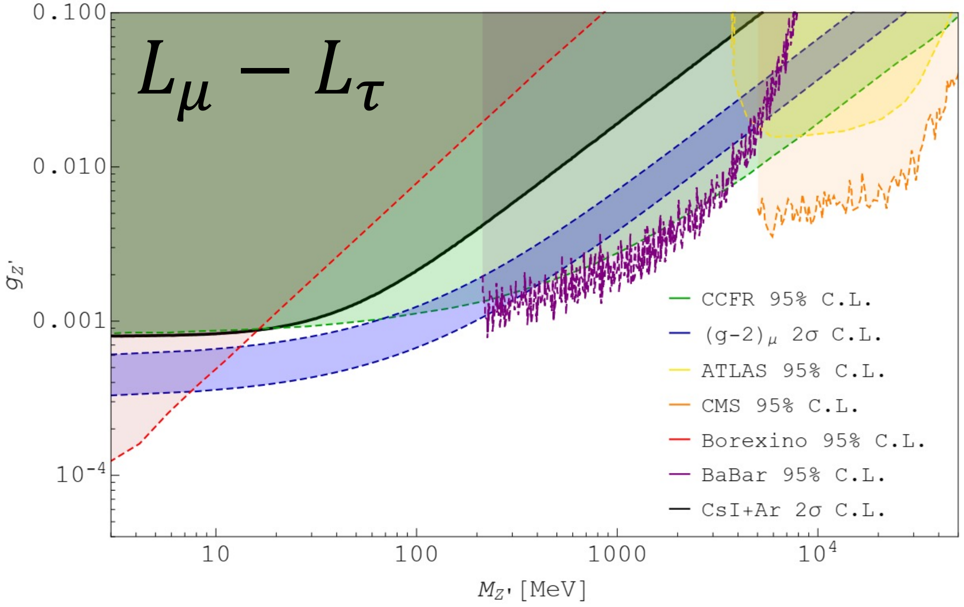

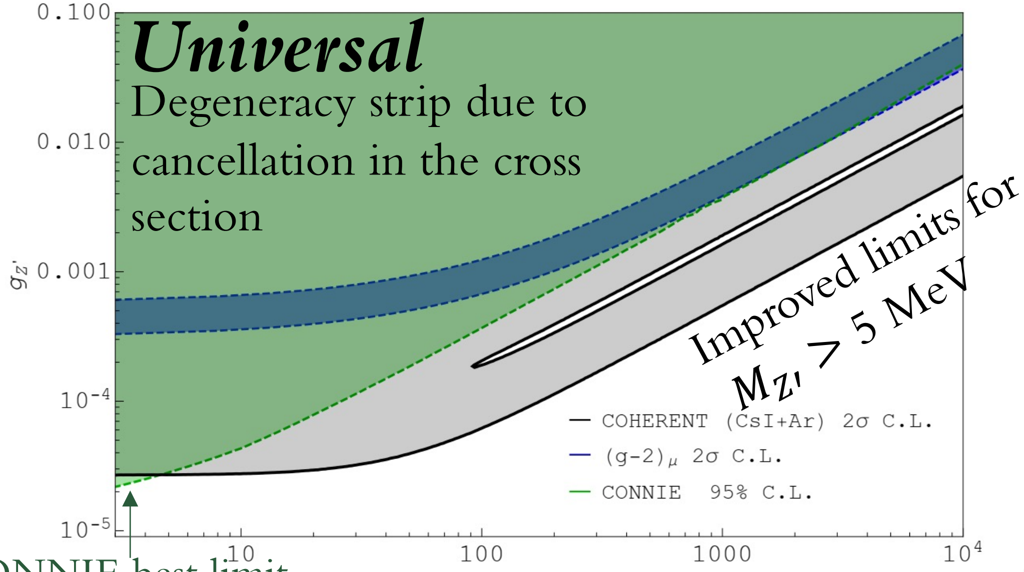

CONNIE best limit for $M_{Z'}<5$ MeV

CONNIE, JHEP 04 (2020) 054

For scalar mediators: Miranda et al, JHEP 05 (2020) 130
(Backup)

HEAVY MEDIATORS

New ν interaction

Updated CsI data improves upon previous constraints

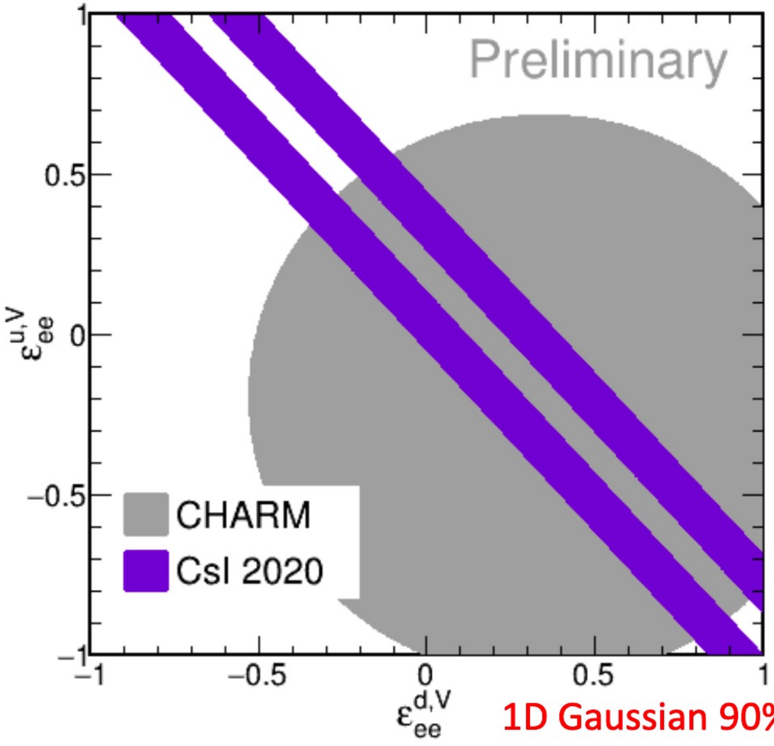

Pershey, talk @Magnificent CEνNS '20

1D Gaussian 90% critical up-values

Combined analysis with ν oscillation data available

P. Coloma et al, JHEP 01 (2021) 114

Comparison with oscillation data:

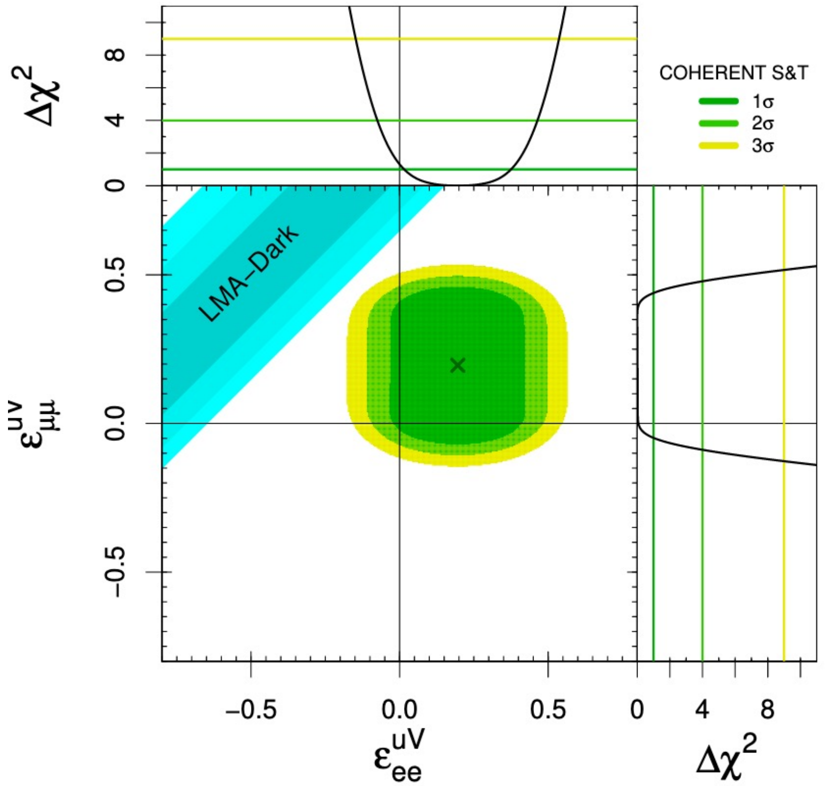

C. Giunti, PRD 101, 035039 (2020)

Degeneracy: $\Delta m^2_{31} \rightarrow -\Delta m^2_{31} + \Delta m^2_{21} = -\Delta m^2_{32}$

$\sin\theta_{12} \rightarrow \cos\theta_{12}\ , \delta \rightarrow \pi - \delta$

+ change in NSI parameters

See also:
P. Coloma et al, PRD 96, 115007 (2017)
Denton at al., arXiv: 1804.03660
Denton and Gehrlein, JHEP 04 (2021) 266
J. Barranco et al, JHEP 0512:021 (2005)
Dutta et al., JHEP 2020, 106 (2020)

New ν properties

ELECTROMAGNETIC INTERACTIONS

For ν's the electric charge is zero and there are ***no electromagnetic interactions at tree level***. However, such interactions can arise from loop diagrams at higher orders of the perturbative expansion of the interaction.

- ***Effective Hamiltonian*** $\mathcal{H}_{em}^{(\nu)}(x) = j_\mu^{(\nu)}(x) A^\mu(x) = \sum_{k,j=1} \overline{\nu_k}(x) \Lambda_\mu^{kj} \nu_j(x) A^\mu(x)$

- We are interested in the neutrino part of the amplitude which is given by the following matrix element $\langle \nu_f(p_f) | j_\mu^{(\nu)}(0) | \nu_i(p_i) \rangle = \overline{u_f}(p_f) \Lambda_\mu^{fi}(q) u_i(p_i)$

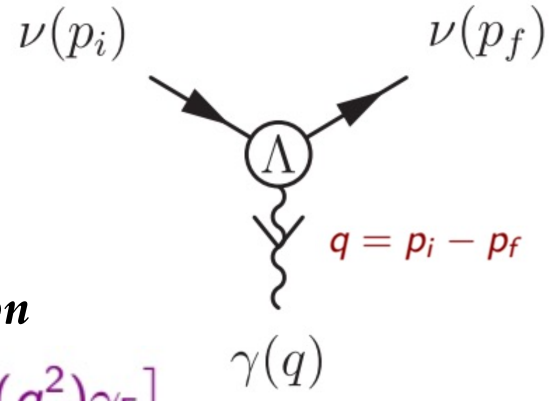

- The electromagnetic properties of neutrinos are embedded by the ***vertex function***

$$\Lambda_\mu(q) = (\gamma_\mu - q_\mu \not{q}/q^2)\left[F_Q(q^2) + F_A(q^2) q^2 \gamma_5\right] - i\sigma_{\mu\nu} q^\nu \left[F_M(q^2) + i F_E(q^2)\gamma_5\right]$$

Lorentz-invariant form factors: charge (F_Q), anapole (F_A), magnetic (F_M), electric (F_E)

$q^2 = 0 \Longrightarrow$ $\mathbb{q}$, a, μ, ε

Charge and anapole moment ($\mathbb{q}$, a) — Magnetic and electric dipole moments (μ, ε)

C. Giunti, A. Studenikin, Rev Mod Phys, 87, 531 (2015)

NEUTRINO CHARGE RADIUS

New ν properties

- In the SM the effective vertex reduces to $\gamma_\mu F(q^2)$ since the contribution $q_\mu \gamma^\mu q_\mu / q^2$ vanishes in the coupling with a conserved current

$$\Lambda_\mu(q) = (\gamma_\mu - q_\mu \gamma^\mu q_\mu / q^2) F(q^2) \cong \gamma_\mu F(q^2)$$

$$F(q^2) = \cancel{F(0)} + q^2 \left.\frac{dF(q^2)}{dq^2}\right|_{q^2=0} + \cdots = q^2 \frac{\langle r^2 \rangle}{6} + \cdots$$

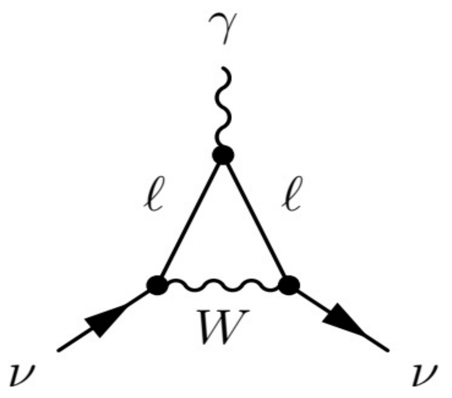

- In the Standard Model $\langle r^2_{\nu_\ell} \rangle_{SM} = -\frac{G_F}{2\sqrt{2}\pi^2}\left[3 - 2\log\left(\frac{m_\ell^2}{m_W^2}\right)\right]$

$\langle r^2_{\nu_e} \rangle_{SM} = -8.2 \times 10^{-33}\ \text{cm}^2$

$\langle r^2_{\nu_\mu} \rangle_{SM} = -4.8 \times 10^{-33}\ \text{cm}^2$

$\langle r^2_{\nu_\tau} \rangle_{SM} = -3.0 \times 10^{-33}\ \text{cm}^2$

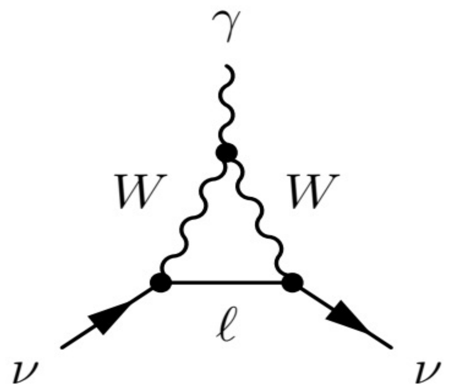

"A charge radius that is gauge-independent, finite is achieved by including additional diagrams in the calculation of $F(q^2)$"

[Bernabeu et al, PRD 62 (2000) 113012, NPB 680 (2004) 450]

New ν properties

NEUTRINO PROPERTIES

Cadeddu et al, PRD 102, 015030 (2020)
Cadeddu et al, PRD 101, 033004 (2020)

ν charge radii

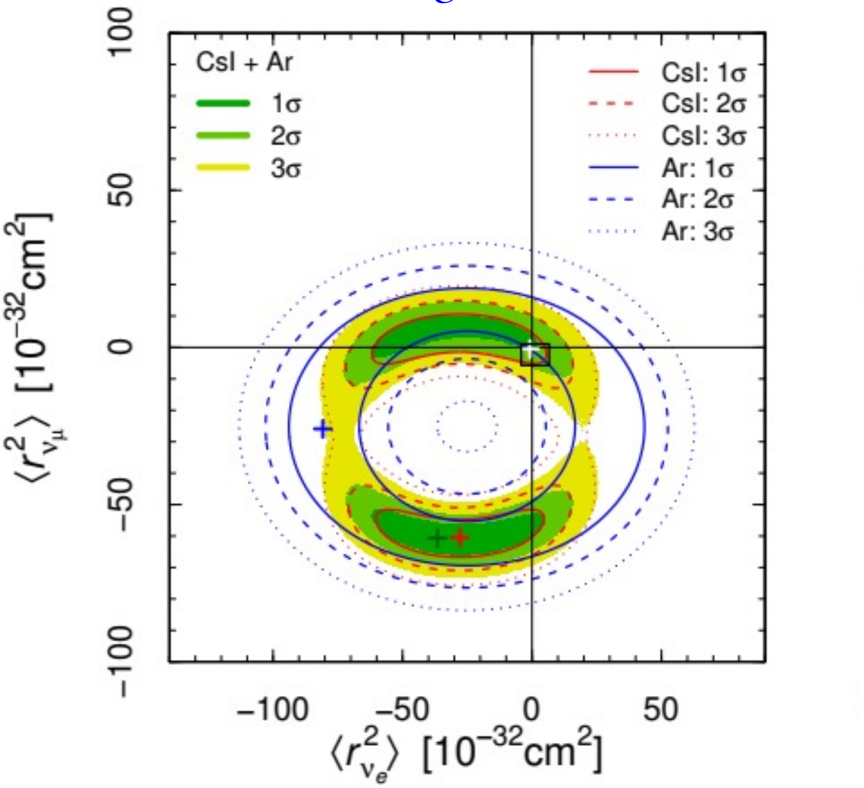

ν millicharges

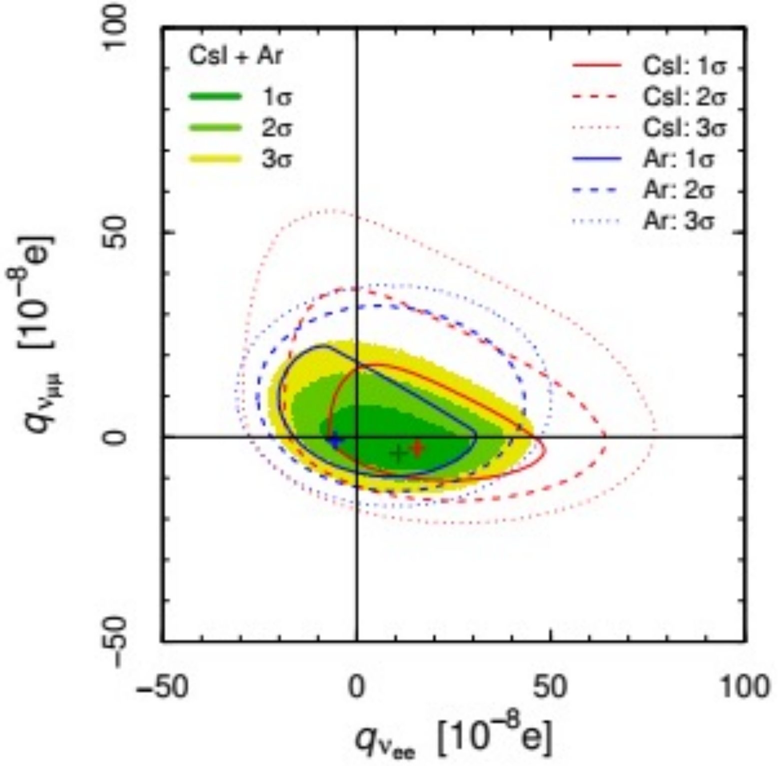

ν magnetic moments

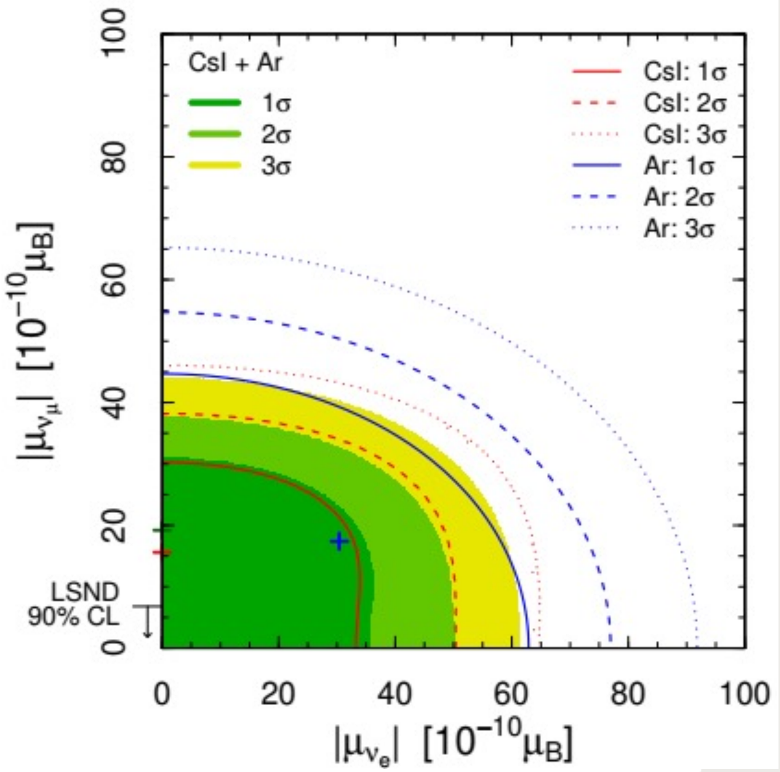

- obtain constraints on the neutrino charge radii:
  $$-78 < \langle r^2_{\nu_e} \rangle < 22, -71 < \langle r^2_{\nu_\mu} \rangle < 17 \times 10^{-32}\ \mathrm{cm}^2.$$
- obtain constraints on the neutrino millicharge :
  $$-20 < q_{\nu_e} < 42, -12 < q_{\nu_\mu} < 20 \times 10^{-8}\ e.$$
- obtain the constraints on the effective neutrino magnetic moment:
  $$|\mu_{\nu_e}| < 56, |\mu_{\nu_u}| < 41 \times 10^{-10} \mu_B$$
- Better constraints from reactor & accelerator experiments

- Argon data more sensitive to the neutrino electric charges because of the lower nuclear mass.
- Only existing laboratory bound of $q_{\nu_{\mu\mu}}$.

- Muon neutrino magnetic moment only about five times larger than the best current laboratory limit (Borexino and red giants).

See also Miranda et al, JHEP 05 (2020) 130
(Backup)

THAT'S NOT ALL FOLKS!

Dark Matter

- Discovery potential for DM from the decay of a dark photon and subsequent DM recoil in COHERENT

  Dutta et al., PRL124, 121802 (2020)
  COHERENT, PRD 102, 052007 (2020)

- Determination of the ν floor for DM experiments

  Bohem et al., arXiv: 1809.06385 (2018)

- Low-mass DM searches

Axion searches

- Production of ALPs by the γ-ray flux of reactors and detection in low-thr detectors close by

  Dent et al., PRL 124.211804
  Sierra et al., arXiv:2010.15712

Supernova neutrinos

- Opacity source for SN ν
- CEνNS as a mean to detect SN ν

  Horowitz et al., PRD 68, 023005
  DarkSide-20k, JCAP03(2021)043

Sterile neutrinos

- Mechanism for probing sterile ν oscillations

  Formaggio et al., PRD 85, 013009 (2012)
  Blanco et al., PRD 101, 075051 (2020)
  Miranda et al., PRD 102, 113014 (2020)

CONCLUSIONS

- CEνNS observation has opened a fantastic window to a plethora of physics observables.
- From an experimental point of view exciting moment: new results by several collaborations expected soon.
- Large and growing interest in the theory community,
- Application to many different areas of particle and nuclear physics and possibilities to explore complementarity between different sectors.

BACKUP SLIDES

REACTOR VS STOPPED-PION AS SOURCES

Source	Flux/ ν's per s	Flavor	Energy	Pros	Cons
Reactor 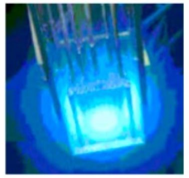	2e20 per GW	nuebar	few MeV	• huge flux	• lower xscn • require very low threshold • CW
Stopped pion 	1e15	numu/ nue/ nuebar	0-50 MeV	• higher xscn • higher energy recoils • pulsed beam for bg rejection • multiple flavors	• lower flux • potential fast neutron in-time bg

From K. Scholberg

FLUX FROM SNS

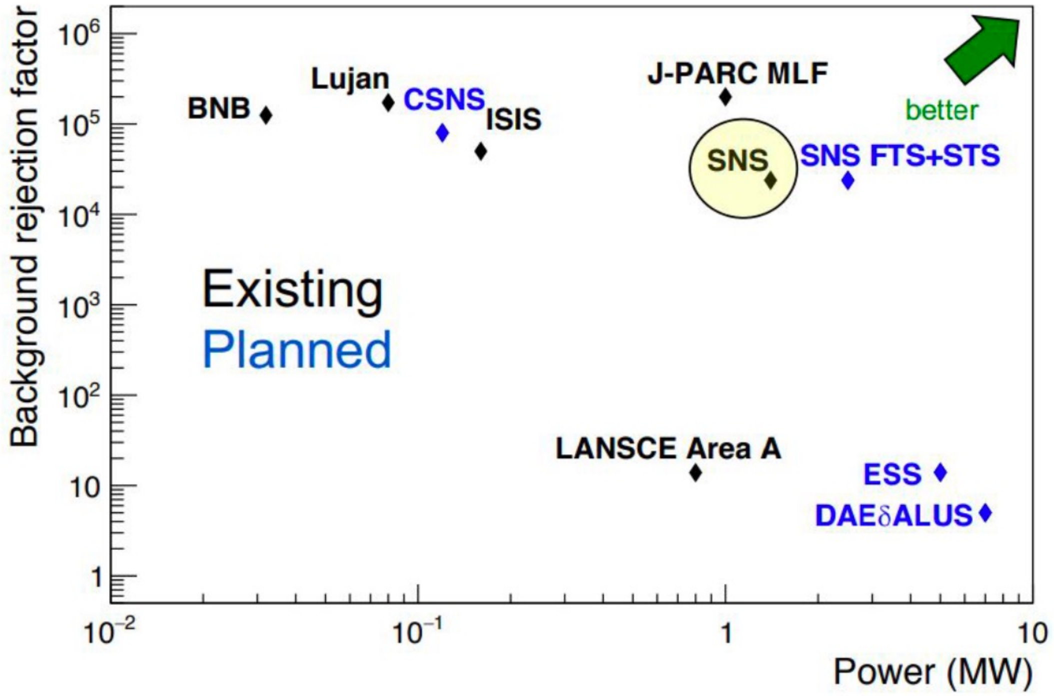

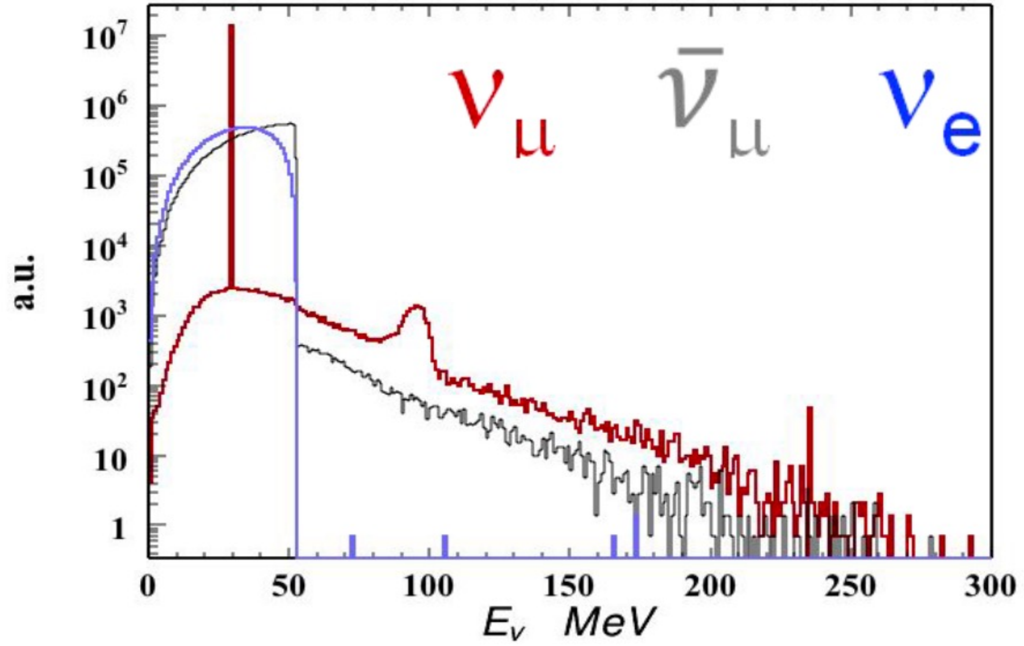

32

NEUTRON FORM FACTOR PARAMETRIZATION

1. ***Symmetrized Two-parameter Fermi form factor***

$$\rho_{SF}(r) = \rho_F(r) + \rho_{SF}(-r) - 1 \text{ with } \rho_F(r) = \frac{\rho_0}{1 + e^{(r-c)/a}}$$

Neutron rms radius

$$R_n^2 = \frac{3}{5}c^2 + \frac{7}{5}(\pi a)^2.$$

$$F_Z^{SF}(q^2) = \frac{3}{qc\left[(qc)^2 + (\pi qa)^2\right]}\left[\frac{\pi qa}{\sinh(\pi qa)}\right] \times \left[\frac{\pi qa \sin(qc)}{\tanh(\pi qa)} - qc\cos(qc)\right].$$

2. ***Helm form factor***

Neutron rms radius

The Helm FF is defined as the product of two fairly simple form factors: one associated with a uniform (box) density F_B and the other one accounting for a Gaussian falloff F_G

$$F_H(q) = F_B(q)F_G(q) = 3\,\frac{j_1(qR_0)}{qR_0}e^{-q^2 s^2/2}$$

$$F_B(q) = \int e^{-i\mathbf{q}\cdot\mathbf{r}}\rho_B(r)d^3r = \int e^{-i\mathbf{q}\cdot\mathbf{r}}\left(\frac{3\Theta(R_0 - r)}{4\pi R_0^3}\right)d^3r = 3\,\frac{j_1(qR_0)}{qR_0}$$

$$F_G(q) = \int e^{-i\mathbf{q}\cdot\mathbf{r}}\rho_G(r)d^3r = \int e^{-i\mathbf{q}\cdot\mathbf{r}}\left(\frac{e^{-r^2/(2s^2)}}{(2\pi s^2)^{3/2}}\right)d^3r = e^{-q^2 s^2/2}.$$

FORM FACTOR

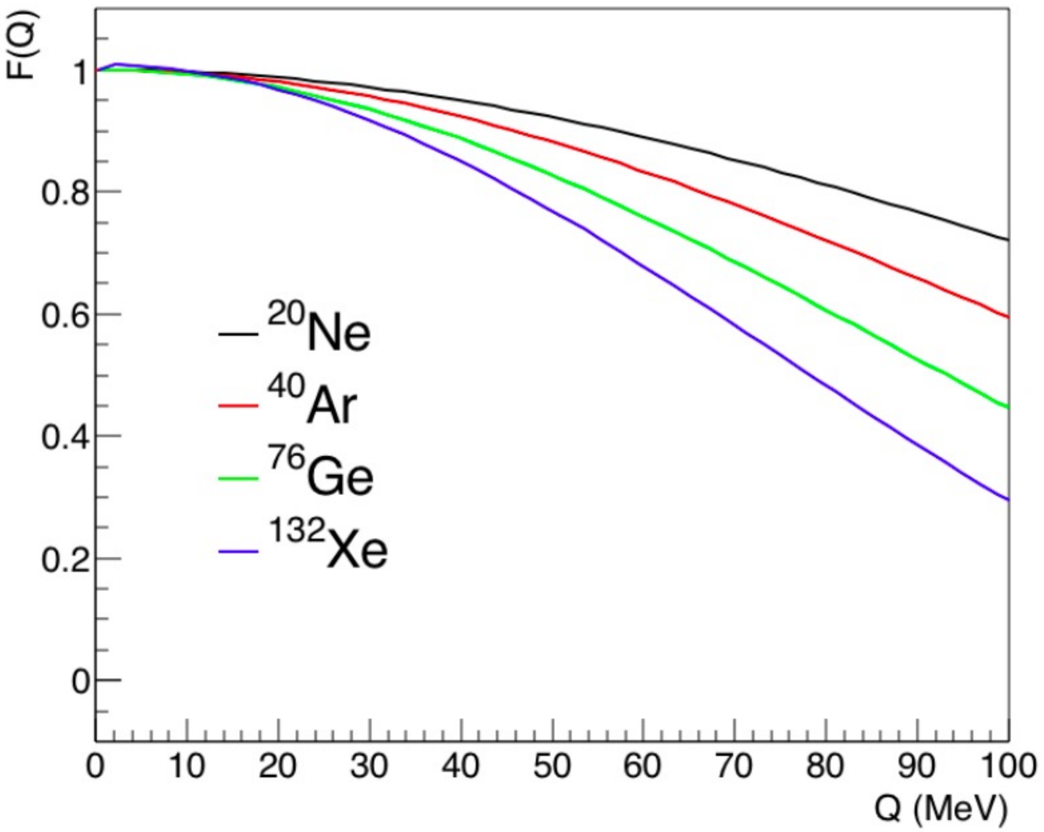

form factor suppresses cross section at large Q

CsI 2020 VS 2017

COHERENT Collaboration, talks @Magnificent CEνNS '20

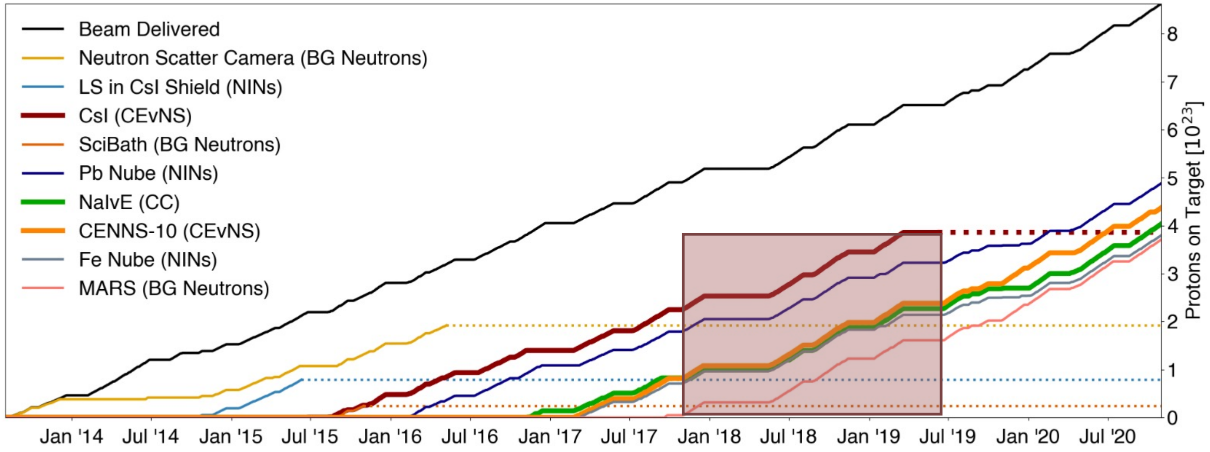

- Increased statistics. More than 2x!
- On June 10, 2019 the detector has been decommissioned.

Improved systematics and re-analysis of the ***quenching factor***: ratio between the scintillation light emitted in nuclear and electron recoils, that determines the relation between the number of detected photoelectrons and the nuclear recoil kinetic energy

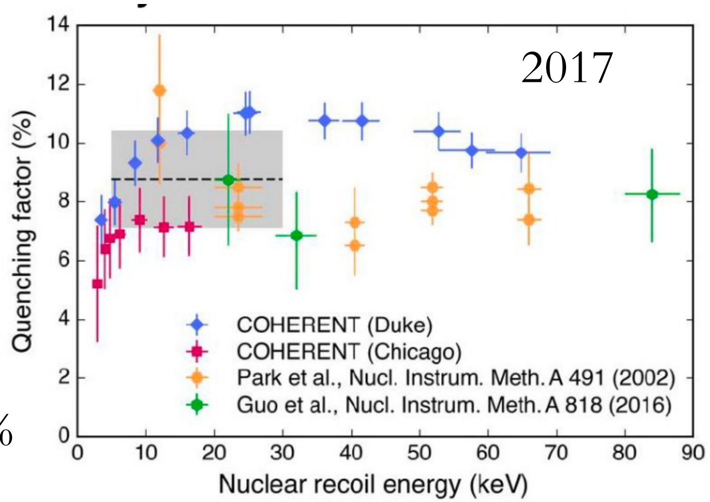

Systematics: 25%

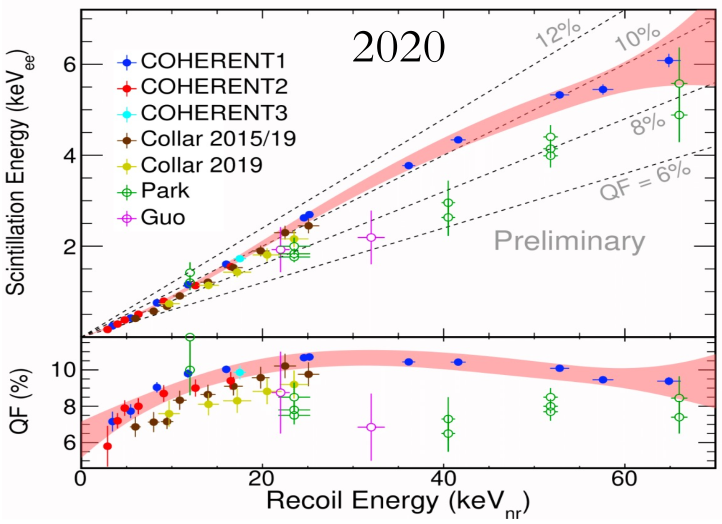

Systematics: 3.6%

EXTRAPOLATED VALUE Δr_{np}^{Cs}

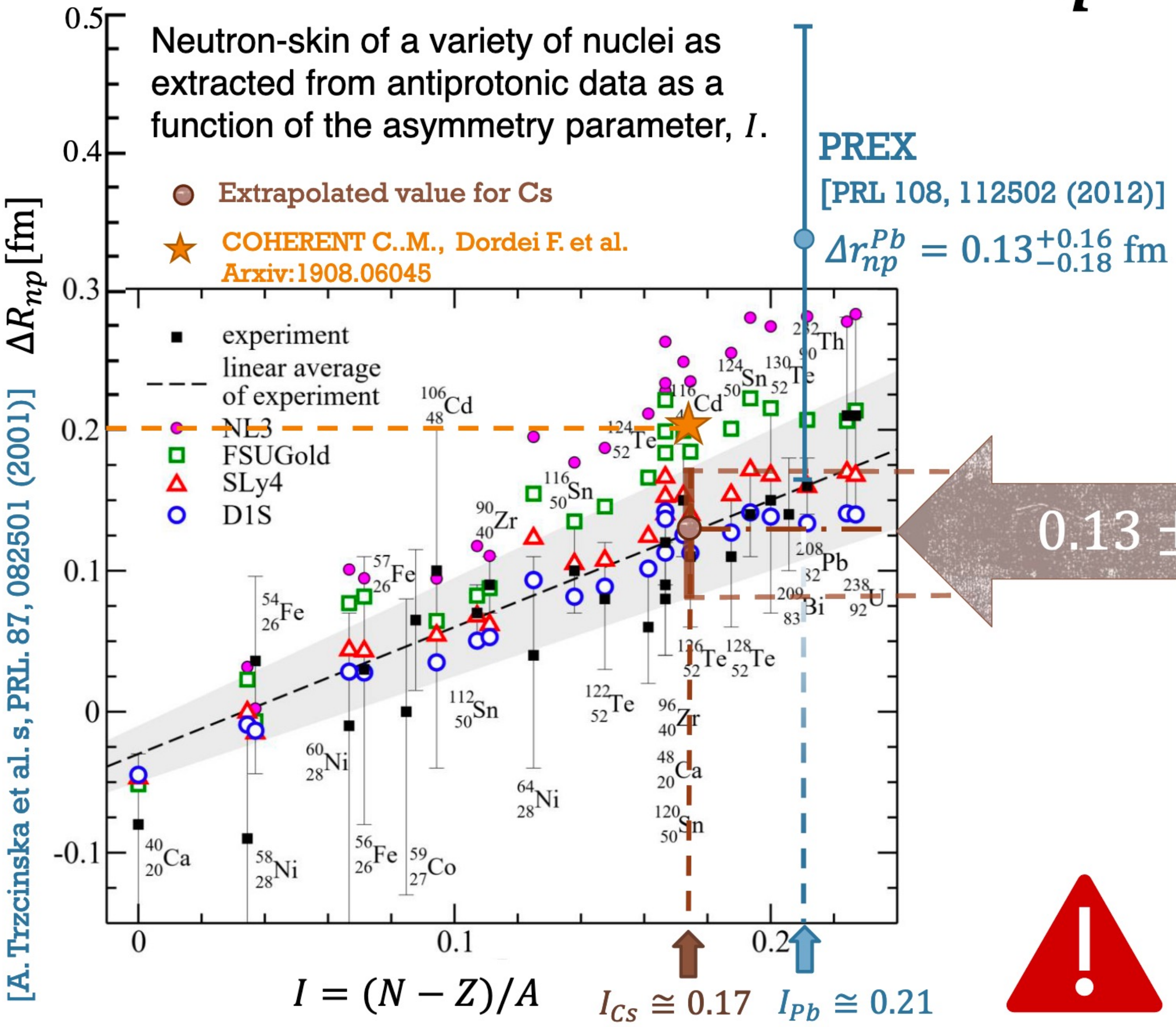

0.13 ± 0.04 fm $\equiv \Delta R_{np}^{Cs}$

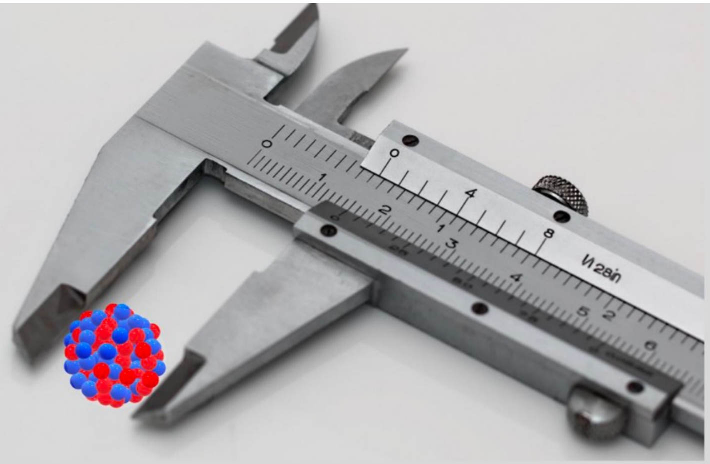

- The red triangles represent a semi-empirical formula derived using the nuclear droplet model:

$$\Delta R_{np}[\text{fm}] = -(0.04 \pm 0.03) + (1.01 \pm 0.15)\frac{N-Z}{A}$$

Extrapolated (not measured) value for Cesium!

Antiprotonic data: radiochemical and the other based on x-ray data constraining the neutron distribution at the nuclear periphery

[Thiel M. et al., Journal of Physics G, 46, 9 (2019), arXiv:1904.12269v1]

"[…] Thus, we must conclude that processes involving hadronic probes tend to grossly underestimate the many sources of theoretical uncertainties."

11

36

From M. Cadeddu, Magnificent CEvNS 2019

COHERENT AND PREX

Cadeddu et al., arXiv:2102.06153

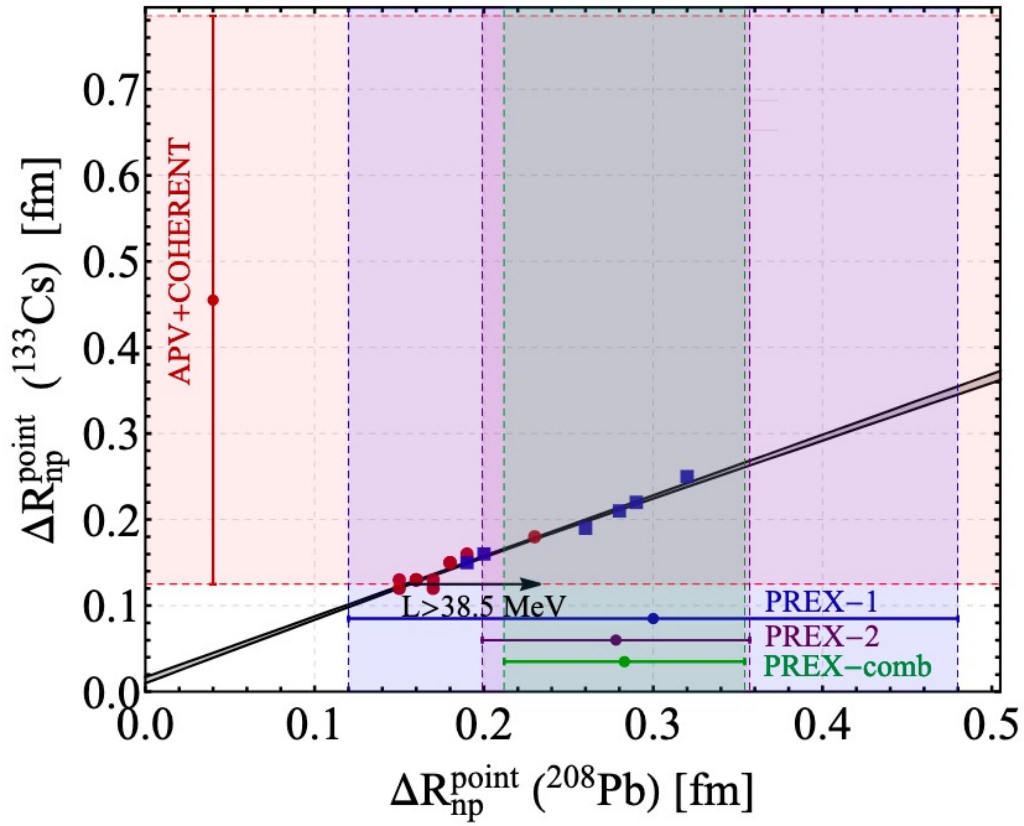

PREX: parity-violating asymmetry *APV* in the elastic scattering of longitudinally polarized electrons from ^{208}Pb

$$A_{\rm PV} = \frac{\sigma_R - \sigma_L}{\sigma_R + \sigma_L} \approx \frac{G_F Q^2 |Q_W|}{4\sqrt{2}\,\pi\alpha Z} \frac{F_{\rm W}(Q^2)}{F_{\rm ch}(Q^2)}$$

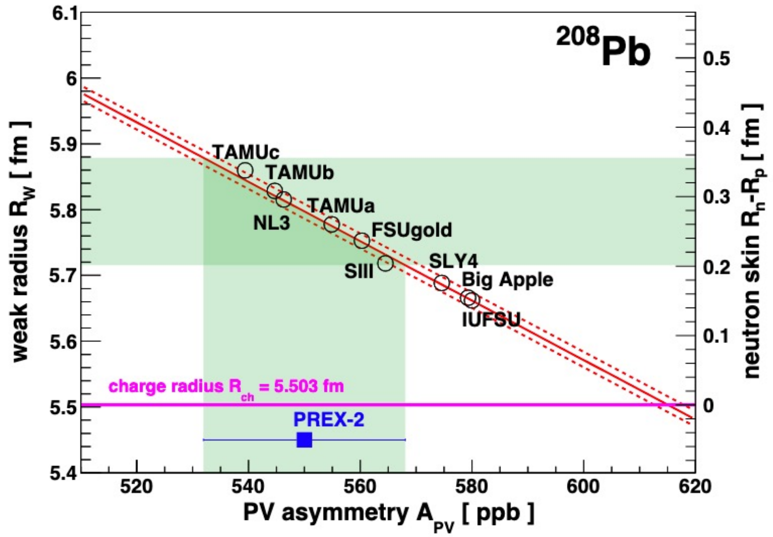

PREX, Phys. Rev. Lett. 126, 172502 (2021)

Reed at al., PRL 126, 172503 (2021)
Horowitz et al., PRL 86, 5647 (2001)
Cadeddu et al., arXiv:2102.06153

IMPLICATIONS OF R_N IN THE ASTROPHYSICAL SECTOR

- The neutron skin of a neutron-rich nucleus is the result of the competition between the Coulomb repulsion between the protons, the surface tension, that decreases when the excess neutrons are pushed to the surface, and the ***symmetry energy***.
- ***symmetry energy:*** reflects the variation in binding energy of the nucleons as a function of the neutron to proton ratio.
- The density dependence of the symmetry energy, that is a fundamental ingredient of the EOS, is expressed in terms of the slope parameter, L, that depends on the derivative of the symmetry energy with respect to density at saturation.

Theoretical calculations show a strong linear correlation between ΔRnp and L, namely larger neutron skins translate into larger values of L

Lower limit for L suggested by the combined COHERENT and APV result

$L > 38.5$ MeV

- given that L is directly proportional to the pressure of pure neutron matter at saturation density, larger values of ΔRnp imply a larger size of neutron stars.

COHERENT UPGRADE

MARS
- Layered plastic scintillator w/ Gd paint
- capture-gated fast n detection

- NaIvE -- 185 kg NaI array
- Test-bed for future ton-scale NaI

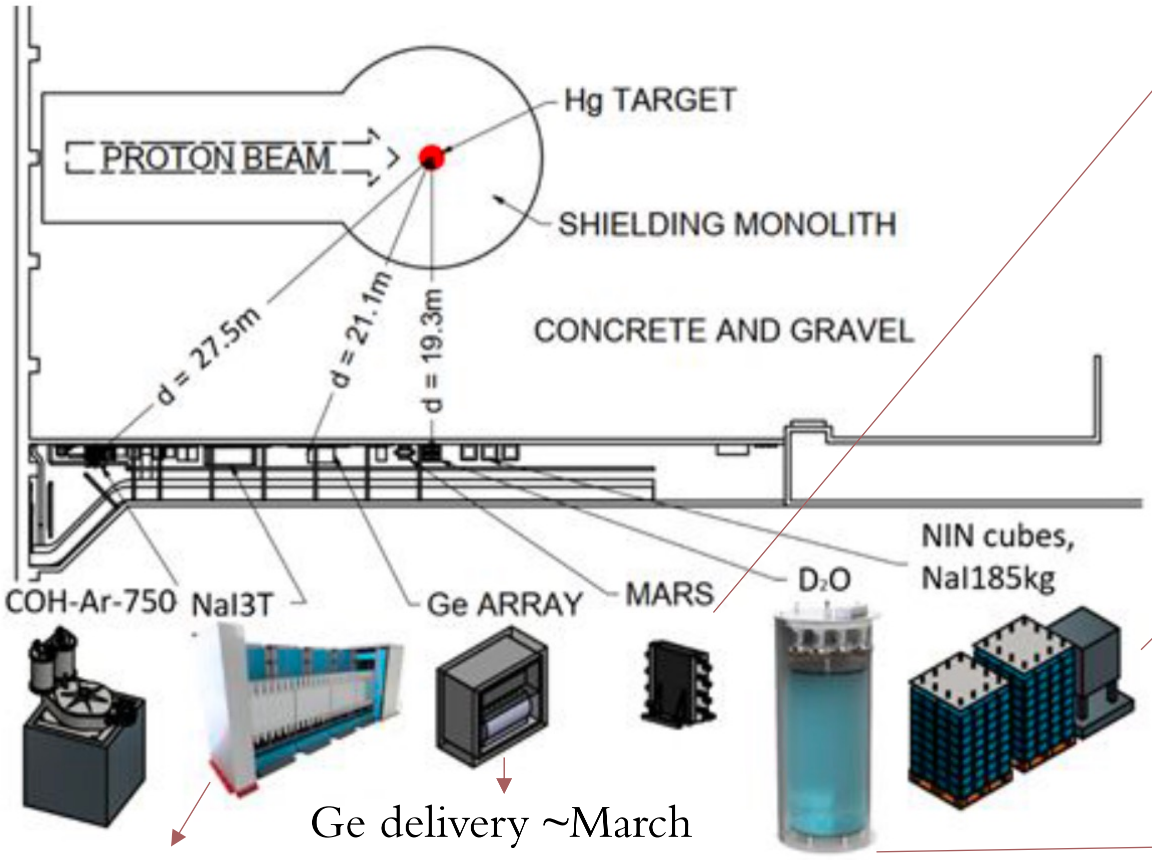

- 610 kg fiducial volume
- 3000 CEvNS per SNS-year
- R&D of cryostat, photodetectors

Finalizing design/shielding

Ge delivery ~March 2021
Commission/acq. summer 2021!

"Neutrino cubes"
- Liquid scintillator surrounded by heavy shielding
- Search for fast n from CC interactions in Pb/Fe/Cu
- Detection scheme for SN ν's

Experiment	Technology	Location
CONUS	HPGe	Germany
Ricochet	Ge, Zn bolometers	France
CONNIE	Si CCDs	Brazil
RED	LXe dual phase	Russia
Nu-Cleus	Cryogenic $CaWO_4$, Al_2O_3 calorimeter array	Europe
MINER	Ge iZIP detectors	USA

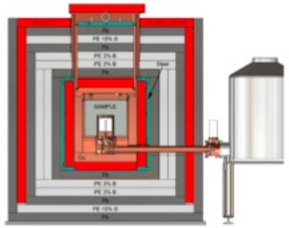

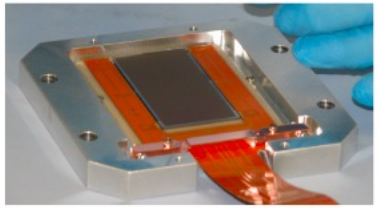
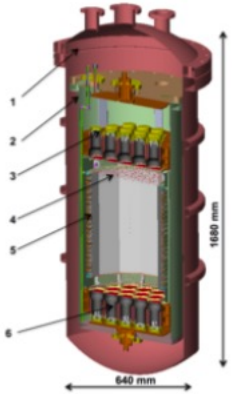
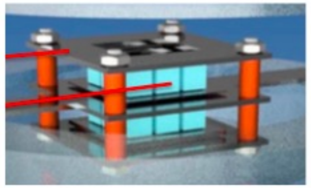


From K. Scholberg

CONNIE EXPERIMENT

- Fully depleted, high resistivity CCDs as particle detectors fabricated on high-resistivity (10-20 kΩ cm) silicon
- Each sensor consists of a square array with 16 millionsquare pixels of 15μm×15μm pitch each
- Close to Angra 2 nuclear power plant (Brazil)
- The engineering proto-type of the experiment was installed at the reactor site in late 2014
- A complete upgrade of the sensors was performed in mid 2016, with the main objective of increasing its active mass by a factor of~40, reaching recoil energies down to 1 keV
- No significant excess of events in the reactor-on minus reactor-off subtraction, strongly limited by the statistics of the reactor-off data.

CONNIE, PRD 100, 092005 (2019)

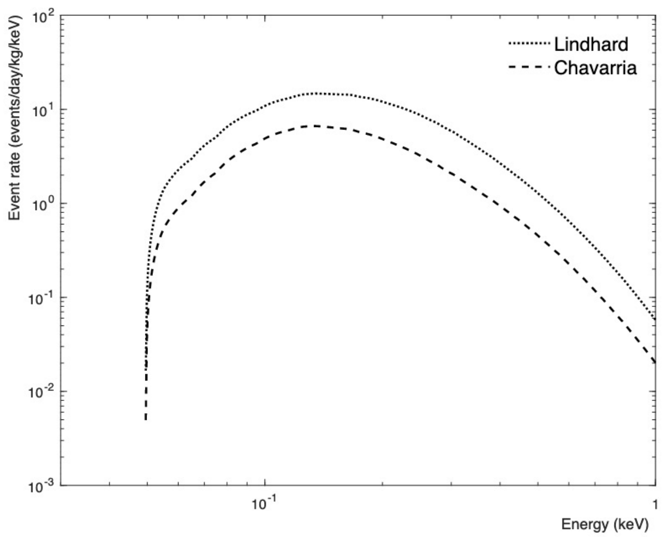

FIG. 17. Observable neutrino recoil spectrum in the CONNIE detector array using two versions of the quenching factor measured from Lindhard et al. [57] (dotted line) and Chavarria et al. [52] (dashed line).

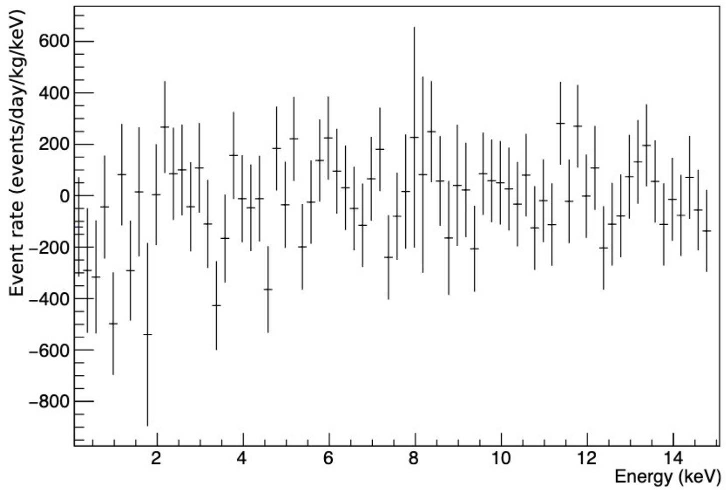

FIG. 19. Energy spectrum difference of reactor-on minus reactor-off data.

NU-CLEUS

- @ a nuclear power reactor (Chooz Nuclear Power Plant) with gram-scale using ultra-low-threshold cryogenic detectors.
- A 0.5 g NUCLEUS prototype detector, operated above ground in 2017, reached an energy threshold for nuclear recoils of below 20 eV
- This sensitivity is achieved with tungsten transition edge sensors which are operating at temperatures of 15 mK and are mainly sensitive to non-thermal phonons.
- The NUCLEUS collaboration is preparing a 10 g array of cryogenic detectors
- The setup is planned to move to Chooz for commissioning in 2021, with data taking expected to start there in early 2022
- Future: R&D effort to upgrade the total mass to 1 kg.

Journal of Low Temperature Physics volume 199, pages 433–440 (2020)

COHERENT @EUROPEAN SPALLATION SOURCE

- ESS will combine the world's most powerful superconducting proton linac with an advanced hydrogen moderator, generating the most intense neutron beams.
- It will also provide an order of magnitude increase in neutrino flux with respect to the SNS

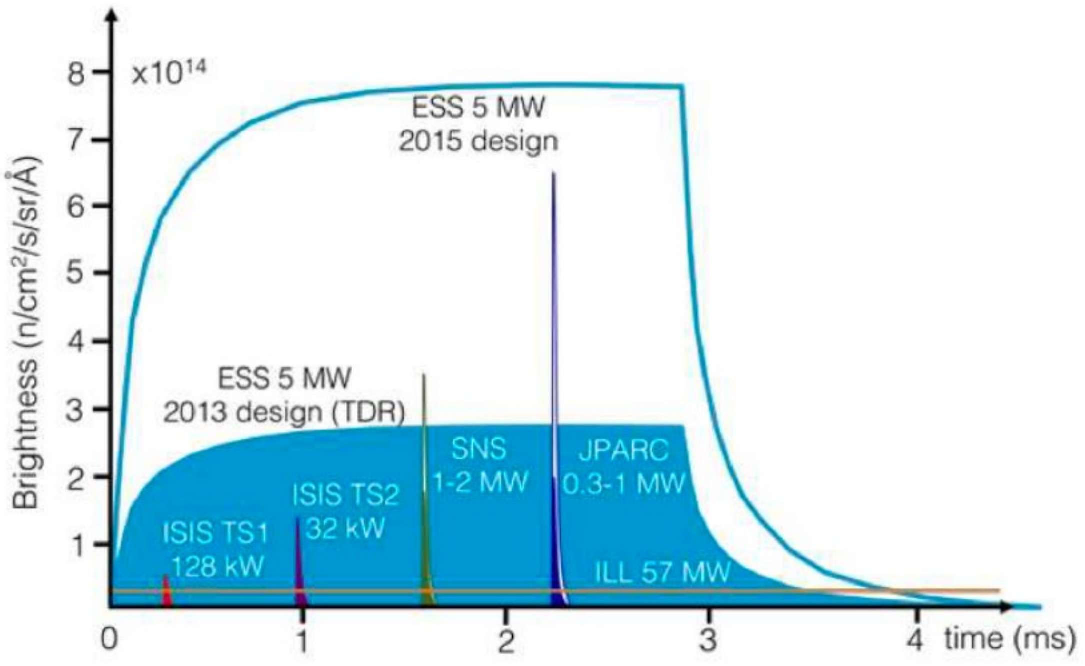

Neutron production from existing and planned spallation sources

- Expected 8.5×10^{22} neutrinos per flavor per year, an order of magnitude higher than the equivalent of 9.2×10^{21} from a reference 1 MW, 0.94 GeV SNS
- Low threshold detectors to increase statistics

JHEP 2020, 123 (2020)

LIGHT MEDIATORS

Scalar mediator scenario:

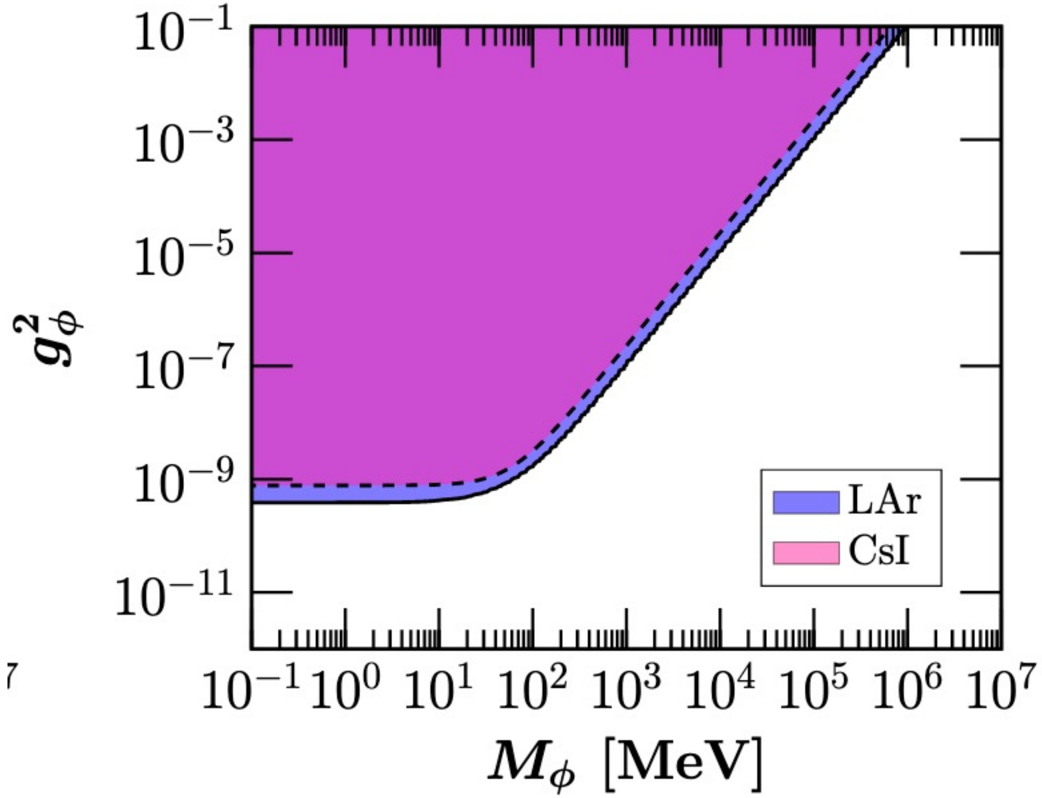

Miranda et al, JHEP 05 (2020) 130

New ν interaction

LIGHT MEDIATORS

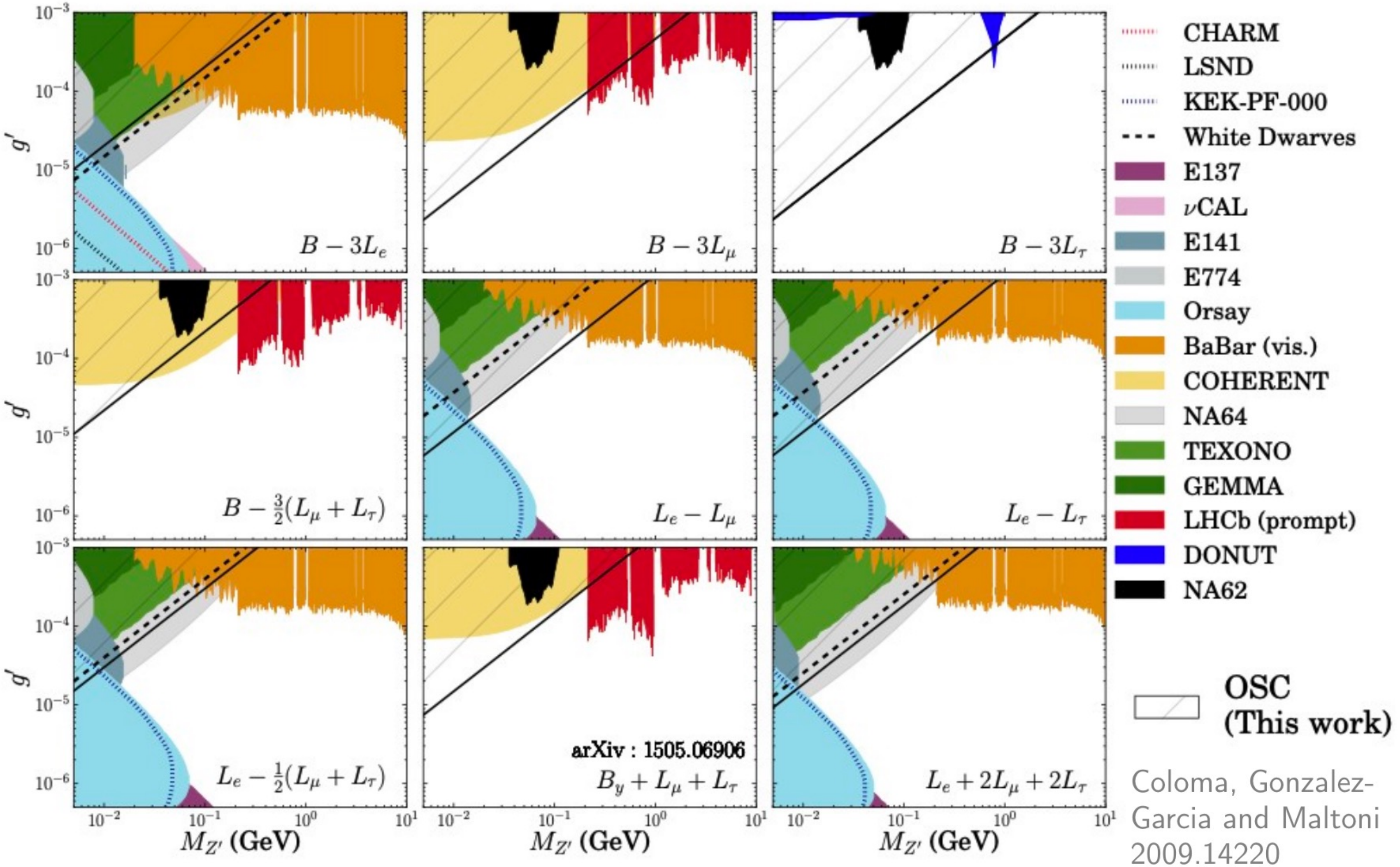

Coloma, Gonzalez-Garcia and Maltoni 2009.14220

From P. Coloma, 3rd Nuclear and Particle Theory meeting 2021

New ν interaction

HEAVY MEDIATORS

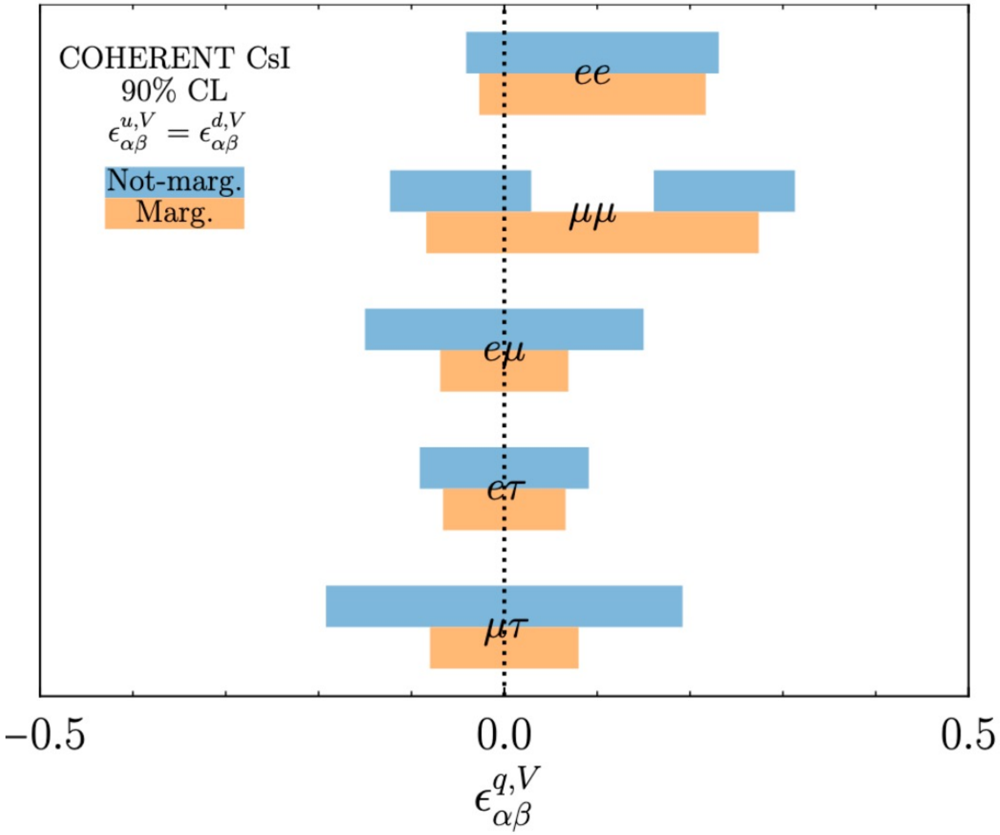

Denton and Gehrlein, JHEP 04 (2021) 266

Comparison with oscillation data:

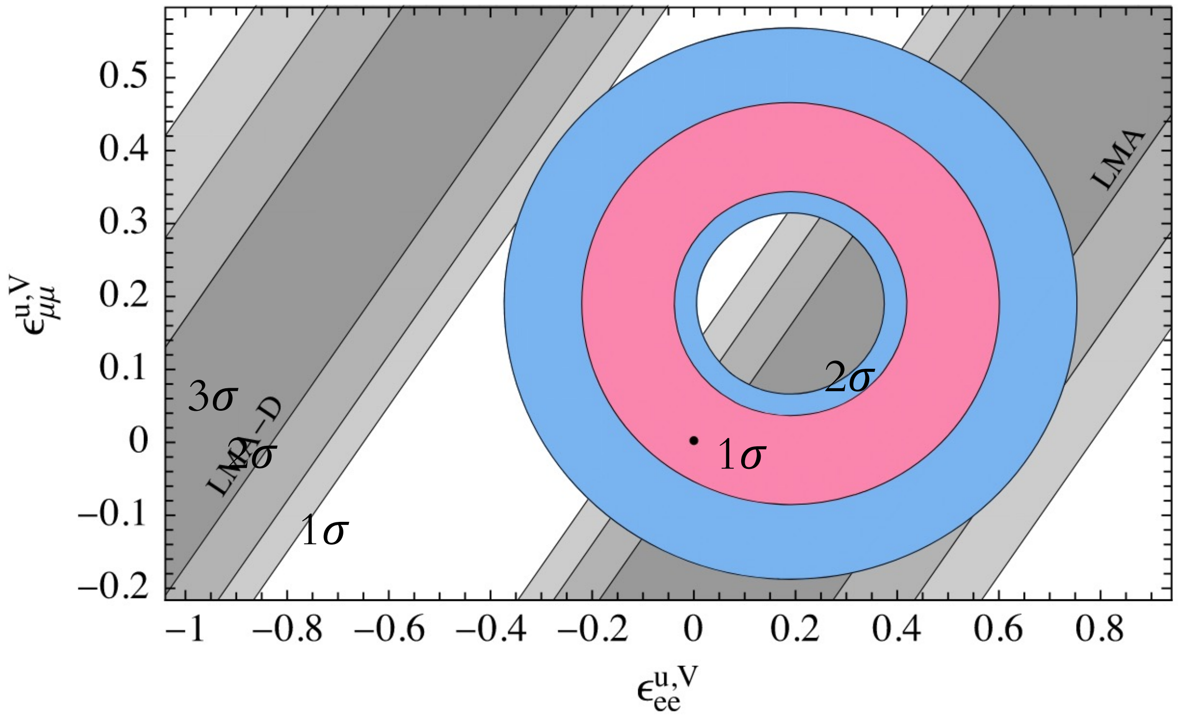

P. Coloma et al, PRD 96, 115007 (2017)

Degeneracy: $\Delta m^2_{31} \to -\Delta m^2_{31} + \Delta m^2_{21} = -\Delta m^2_{32}$

$\sin\theta_{12} \to \cos\theta_{12}$, $\delta \to \pi - \delta$

+ change in NSI parameters

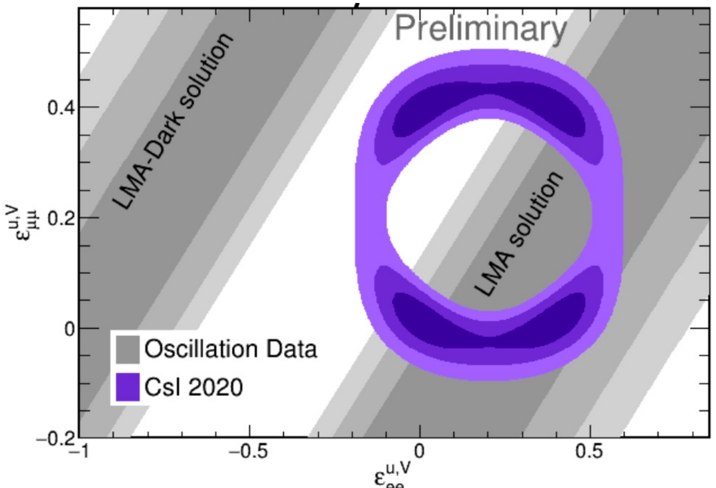

Pershey, talk @Magnificent CEνNS '20

Combined analysis with ν oscillation data available

P. Coloma et al, JHEP 01 (2021) 114

ATOMIC PARITY VIOLATION* ON Cs

*also known as PNC (Parity nonconservation)

- In the absence of electric fields and weak neutral currents, **an electric dipole** (E1) transition between two atomic states with same parity (6S and 7S in Cs) is forbidden by the parity selection rule.
- However an electric dipole transition amplitude can be induced by a Z boson exchange between atomic electrons and nucleons → Atomic Parity Violation (APV)

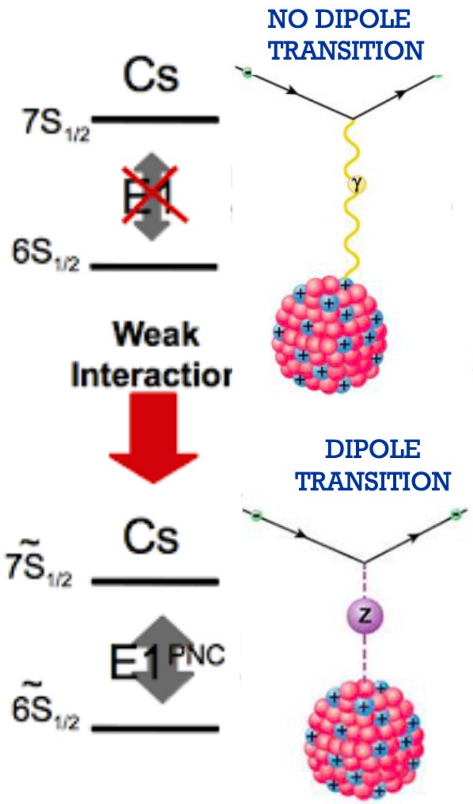

- ➢ The weak NC interaction violates parity and mixes a small amount of the P state into the 6S and 7S states ($\sim 10^{-11}$), characterized by the quantity $\mathbf{Im}(\boldsymbol{E1_{PNC}})$, giving rise to a 7S → 6S transition.

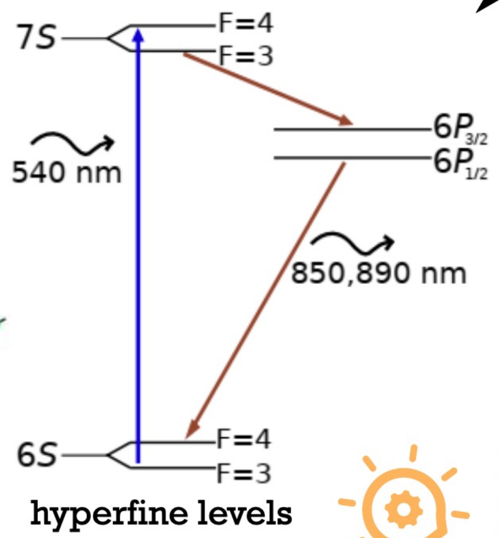

- ➢ To obtain an observable that is at first order in this amplitude, an electric field **E** (that also mixes S & P) is applied. **E** gives rise to a "**Stark induced**" E1 transition amplitude, $\mathbf{A_E}$ that is typically 10^5 times larger than $\mathbf{A_{PNC}}$ and can **interfere** with it.

$$R_{7S\rightarrow 6S} = |A_E \pm A_{PNC}|^2 =$$
$$= \boldsymbol{E1_\beta}^2 \pm 2\boldsymbol{E1_\beta}\boldsymbol{E1_{PNC}} + E_{PNC}{}^2$$

Because the interference term is linear in $\boldsymbol{E1_{PNC}}$ it can be large enough to be measured, but it must be distinguished from the large background contribution ($E1_\beta{}^2$).

7

From M. Cadeddu, Magnificent CEvNS 2019

THE EXPERIMENTAL TECHNIQUE

For there to be a nonzero interference term, **the experiment must have a "handedness",** and if the handedness is reversed, the interference term will change sign, and can thereby be distinguished as a modulation in the transition rate

$$R_{7S\to 6S} = |A_E \pm A_{PNC}|^2 \simeq E1_\beta{}^2 \pm 2\boldsymbol{E1_\beta E1_{PNC}}$$

- **Stark-interference technique**: cesium atoms pass through a region of perpendicular electric, magnetic, and laser fields. The "handedness" of the experiment is changed by reversing the direction of all fields.

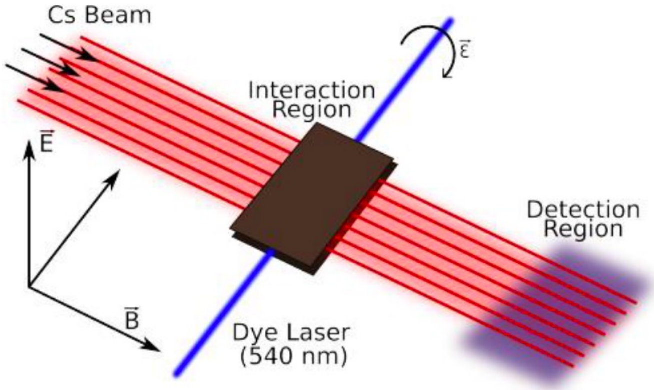

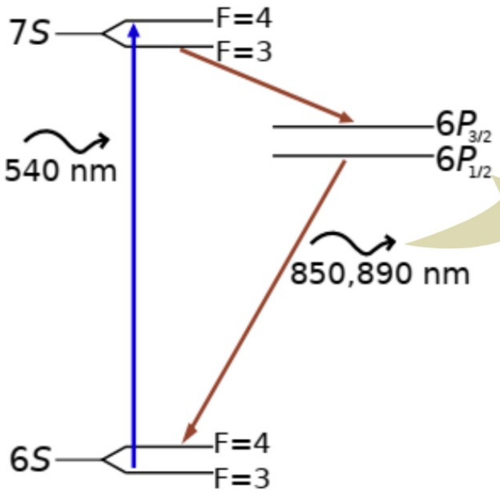

The transition rate is obtained by measuring the amount of 850- and 890-nm light emitted in the 6*P*-6*S* step of the 7*S*-6*S* decay sequence.

✓ The measurements culminated in 1997 when the Boulder group performed a measurement of A_{PNC}/A_E with an uncertainty of just 0.35%.

$$\mathrm{Im}\left(\frac{E_{PNC}}{\beta}\right) = -1.5935(56)\ \frac{\mathrm{mV}}{\mathrm{cm}}$$

[C. S. Wood et al., Science **275**, 1759 (1997)]

The PV amplitude is in units of the equivalent electric field required to give the same mixing of *S* and *P*states as the PV interaction

[Roberts et al., Annu. Rev. Nucl. Part. Sci. 65, 63 (2015)]

8

From M. Cadeddu, Magnificent CEvNS 2019

EXTRACTING THE WEAK CHARGE

$$Q_W = N\left(\frac{\text{Im}\, E_{\text{PNC}}}{\beta}\right)_{\text{exp.}}\left(\frac{Q_W}{N\,\text{Im}\, E_{\text{PNC}}}\right)_{\text{th.}}\beta_{\text{exp.+th.}}$$

Experimental value of electric dipole transition amplitude between 6S and 7S states in Cs

$$-\text{Im}\left(\frac{\mathbf{E_{PNC}}}{\boldsymbol{\beta}}\right) = 1.5935(56)\ \text{mV/cm}$$

[C. S. Wood et al, Science **275**, 1759 (1997)]

Theoretical PNC amplitude of the 6S-7S electric dipole transition

$$E_{\text{PNC}} = \sum_n \left[\frac{\langle 6s|H_{\text{PNC}}|np_{1/2}\rangle\langle np_{1/2}|\mathbf{d}|7s\rangle}{E_{6s}-E_{np_{1/2}}} + \frac{\langle 6s|\mathbf{d}|np_{1/2}\rangle\langle np_{1/2}|H_{\text{PNC}}|7s\rangle}{E_{7s}-E_{np_{1/2}}}\right],$$

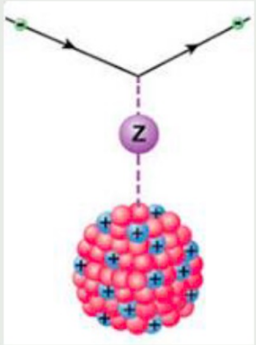

where $\boldsymbol{d}$ is the electric dipole operator, and

$$H_{\text{PNC}} = -\frac{G_F}{2\sqrt{2}} Q_W \gamma_5 \rho(\mathbf{r})$$

is the nuclear spin independent Hamiltonian describing the **electron-nucleus weak interaction**

$\rho(\boldsymbol{r}) = \rho_p(\boldsymbol{r}) = \rho_n(\boldsymbol{r}) \rightarrow$ *neutron skin correction* needed

$\boldsymbol{\beta}$: tensor transition polarizability

It characterizes the size of the Stark mixing induced electric dipole amplitude (external electric field)

[Bennet and Wieman, PRL 82, 2484 (1999)]
[A. Dzuba and V. Flambaum., PRA 62, 052101 (2000)]

$$\beta = 26.957(51)\ a_B^3$$

9

From M. Cadeddu, Magnificent CEvNS 2019

NEUTRINO PROPERTIES

New ν properties

Single energy bin analysis for LAr

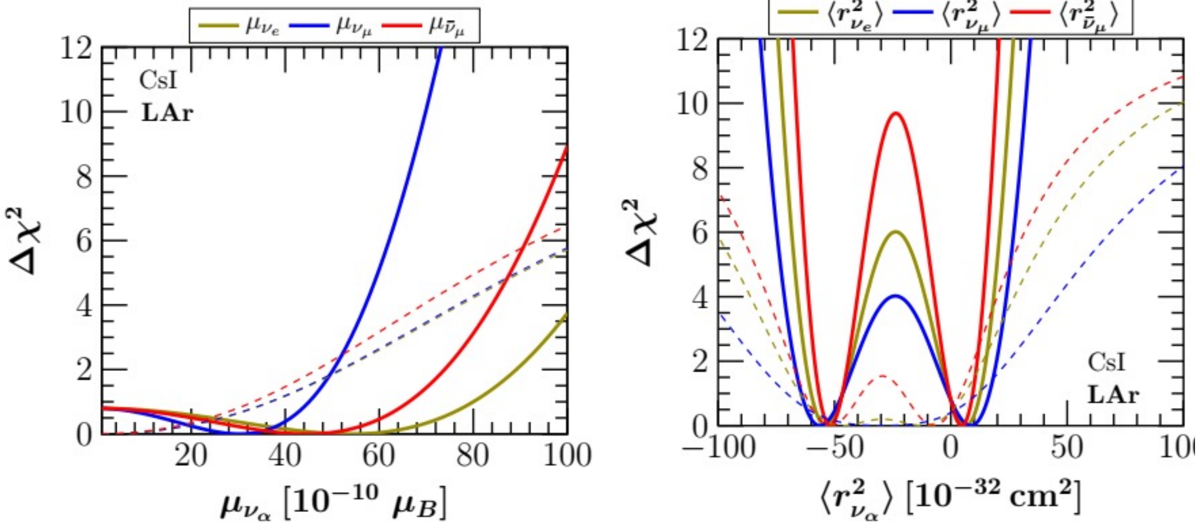

FIG. 5: Sensitivity to the neutrino magnetic moment (left) and charge radius (right). Thick (thin) curves correspond to the LAr (CsI) measurement.

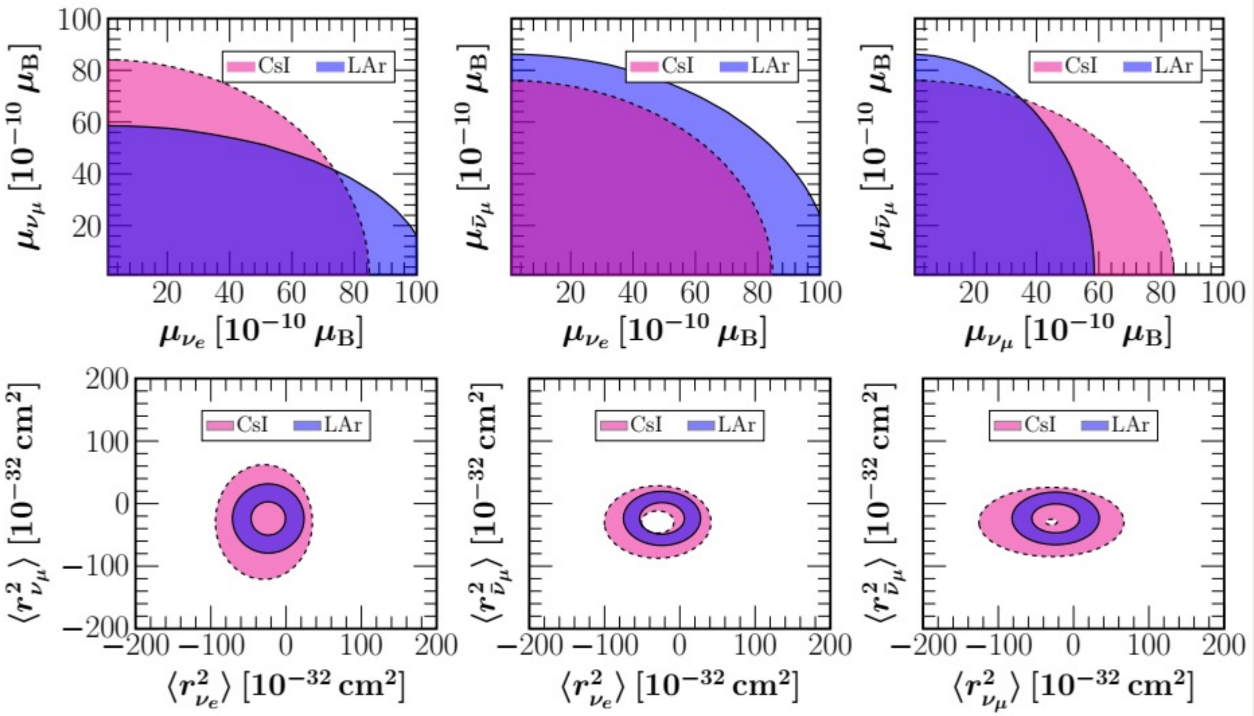

FIG. 6: Upper panel: 90% C.L. allowed region in the parameter space of the neutrino magnetic moments $(\mu_{\nu_\alpha}, \mu_{\nu_\beta})$. Lower panel: 90% C.L. allowed region in the parameter space of neutrino charge radii $(\langle r^2_{\nu_\alpha}\rangle, \langle r^2_{\nu_\beta}\rangle)$. The results are shown for different choices of neutrino flavours, with the undisplayed parameters in each case assumed to be vanishing. For comparison, we show the results from the analysis of CsI and LAr data.

90% C.L.

$$(\mu_{\nu_e}, \mu_{\nu_\mu}, \mu_{\bar{\nu}_\mu}) < (94, 53, 78)\ 10^{-10}\mu_B$$

90% C.L.

$$\langle r^2_{\nu_e}\rangle = (-64, -41) \text{ and } (-7, 16)\,,$$
$$\langle r^2_{\nu_\mu}\rangle = (-69, -37) \text{ and } (-10, 21)\,,$$
$$\langle r^2_{\bar{\nu}_\mu}\rangle = (-60, -43) \text{ and } (-5, 12)\,,$$

in units of 10^{-32}cm^2

Miranda et al, JHEP 05 (2020) 130

LARGE WORLD-WIDE INTEREST IN PURSUING CEνNS

Coherent Elastic Neutrino-Nucleus Scattering: Theoretical and experimental impact

D. Aristizabal Sierra,[1,2] C. Augier,[3] A.B. Balantekin,[4] P. S. Barbeau,[5,6] V. A. Bednyakov,[7] I. A. Bernardi,[8] J. Billard,[3] C. Bonifazi,[9] N. S. Bowden,[10] M. Cadeddu,[11] D. Chernyak,[12] P. Coloma,[13] J. Daughhetee,[8] André de Gouvêa,[14] M. De Jésus,[3] J. B. Dent,[15] P.B. Denton,[16] K. Ding,[12] V. De Romeri,[17] F. Dordei,[11] B. Dutta,[18] Yu. Efremenko,[8] J. Estrada,[19] Y. Farzan,[20] A. Fava,[19] M. Febbraro,[21] G. Fernandez Moroni,[19] E. Figueroa-Feliciano,[22] J. A. Formaggio,[23] A. Galindo-Uribarri,[24] F. Gao,[25] E. A. Garcés,[26] J. Gascon,[3] J. Gehrlein,[16] C. Giunti,[27] M.P. Green,[28,24,6] W. Haxton,[29,30] M.R. Heath,[24] S. Hedges,[5,6] M. Hoferichter,[31] N. Jachowicz,[32] I. Jovanovic,[33] T. Katori,[34] I. Katsioulas,[35] Amir N. Khan,[36] D. Kim,[37] H. Kluck,[38] T.S. Kosmas,[39] N.A Kurinsky,[19] R.F. Lang,[40] S.Y. Lee,[41] B.G. Lenardo,[42] I. Levine,[43] Y. F. Li,[44] J. Liu,[12] L. Li,[5,6] P.A.N. Machado,[19] D.M. Markoff,[45] J. Mattingly,[46] B. Mauri,[47] J. Menéndez,[48] O. G. Miranda,[49] D. V. Naumov,[7] R. Neilson,[50] J. Newby,[21] J.L. Newstead,[51] K. Ni,[52] K. Nikolopoulos,[35] C. Nones,[47] D. Norcini,[53,54] K.J. Palladino,[4] V. Pandey,[55] D.K. Papoulias,[39] A. Parada,[56] J.C. Park,[57] D.S. Parno,[58] L. Pattavina,[59,60] E. Picciau,[61,62] J. Qi,[52] K. Ramanathan,[53,54] R. Rapp,[58] H. Ray,[55] J. Raybern,[5] G.C. Rich,[53] A. Ritz,[63] G. Sanchez Garcia,[49] T. Salagnac,[3] D.J. Salvat,[64] O. Sanders,[49] J. Schieck,[38,65] K. Scholberg,[5] A. Schwenk,[66] S. Shin,[41] I.M. Shoemaker,[67] V. Sibille,[23] N.J.C. Spooner,[68] R. Strauss,[60] L.E. Strigari,[37] B.D. Suh,[64] J. Suhonen,[69] A.M. Suliga,[70] Z. Tabrizi,[67] V. Takhistov,[71] R. Tayloe,[64] M. Toups,[19] M. Tórtola,[17] M. Tripathi,[55] José W. F. Valle,[17] M. Vidal,[72] M. Vignati,[73] M. Vivier,[47] V. Wagner,[60] J. W. Walker,[15] J. Xu,[10] Y. Y. Zhang,[44] and J. Zettlemoyer[64]

We are just at the very beginning of an exciting era in CEνNS research. There is a multi-faceted experimental effort on-going around the world to expand upon the COHERENT measurements and to study CEνNS using different neutrino sources and detector technology both as a means to study the CEνNS interaction itself and to probe other aspects of physics. Given the broad scientific applications of CEνNS, and its complementarity to many different aspects neutrino physics, it will be an important aspect of the neutrino physics program in the coming decade.